**Investigation of Copper(I) Cyanide for Use as a Luminescent Sensor Device**

**A thesis submitted in partial fulfillment of the requirement for the degree of Bachelors of Science in Department of Chemistry from The College of William and Mary**

**by**

**Matthew D. Dembo**

**Accepted for _____**

_____

**Robert D. Pike, Director**

_____

**Gary W. Rice**

_____

**John C. Poutsma**

_____

**John D. Griffin**

**Williamsburg, VA**
**May 2, 2011**

# Investigation of Copper(I) Cyanide for Use as a Luminescent Sensor Device

## TABLE OF CONTENTS

**Acknowledgements**

I would like to thank Dr. Robert D. Pike for vastly refining my proficiency in the laboratory and helping me to develop a keen respect for the scientific process, as well as for his numerous edits to the following publication. You have shown me endless patience and encouraging words when most needed, and I am eternally grateful. I would also send my thanks to Dr. John D. Griffin, who has given me the opportunity to explore another passion of mine. Your zeal is contagious, and I am happy to have pursued a second degree in Neuroscience because of it. I give my thanks to Dr. Gary W. Rice for reminding me that there's more to life than just work, and to Dr. John C. Poutsma for always bringing a good sense of humor. Furthermore, I thank the aforementioned committee for your time and consideration in the review of this thesis. Finally, I would like to show my gratitude to the National Science Foundation (CHE-0848109) for supporting this work.

## List of Figures

*Figure* *Page*

## List of Tables and Schemes

*Table* *Page*



*Scheme* *Page*

## Abstract

An investigation of the synthesis and luminescent properties of copper(I) cyanide metal-organic networks containing amine and imine ligands is reported. The development of an ambient temperature synthesis of these networks was explored, with products characterized through a variety of methods. These included Thermogravimetric Analysis (TGA), powder X-ray diffraction (PXRD), fluorimetry, and elemental analysis, among others. These analytical techniques showed neat, ambient temperature synthesis to be a practical alternative to heated reactions for producing more consistent products. Furthermore, the luminescent behavior of CuCN in response to exposure to either liquid or gaseous amines was characterized across several different solid state CuCN morphologies, including powder, compressed pellets, and CuCN impregnated polymer films. The luminescence observations were consistent across all platforms, suggesting that CuCN could serve as a viable foundation for a luminescent sensor of gaseous amines or other volatile organics.

# INTRODUCTION

## Copper(I) Cyanide

Copper(I) salts can be obtained inexpensively and are known to form very stable, simple complexes that are just as strongly emissive as other similar $d^{10}$ Au(I) and Ag(I) complexes, making it a favorite for luminescent study.[1] Copper is a transition metal in Group 11 with closed shell electron configuration [Ar] $3d^{10}4s^{1}$. An electron is transferred from the 4s-orbital to fill the 3d subshell so that each d-orbital is occupied by a pair of opposite-spin electrons. Having a filled d-subshell gives copper(I) the electron configuration [Ar] $3d^{10}$. The full d-subshell supports formation of stable complexes with ligands via π-backbonding. Backbonding ligands both donate to the metal in a sigma sense and receive electron density "back" from the metal into vacant π-orbitals.

Additionally, having filled d-orbitals eliminates any d-d electronic transitions in copper(I) and limits the metal coordination sphere to a maximum of four additional bonds according to the 18-electron rule. Linear two-coordinate, trigonal three-coordinate, and tetrahedral four-coordinate geometries are most frequently observed for copper (I). Since the relatively electron-rich copper metal is limited to low-coordinate complexes, the resulting structures are typically simpler in nature than other higher-coordinating transition metals, making them much less difficult to analyze.[2] An cation with a tetrahedral metal center is shown in Figure 1 below as an example of a four-coordinate copper complex (pmea = 2-(pyridin-2-yl)-N,N-bis(pyridine-2-ylmethyl)ethanamine).

Figure 1: ORTEP Plot of $[Cu(pmea)]^+$ Cation. Thermal ellipsoids are shown at 50% probability with hydrogen atoms and $PF_6$ anion omitted for clarity.[3]

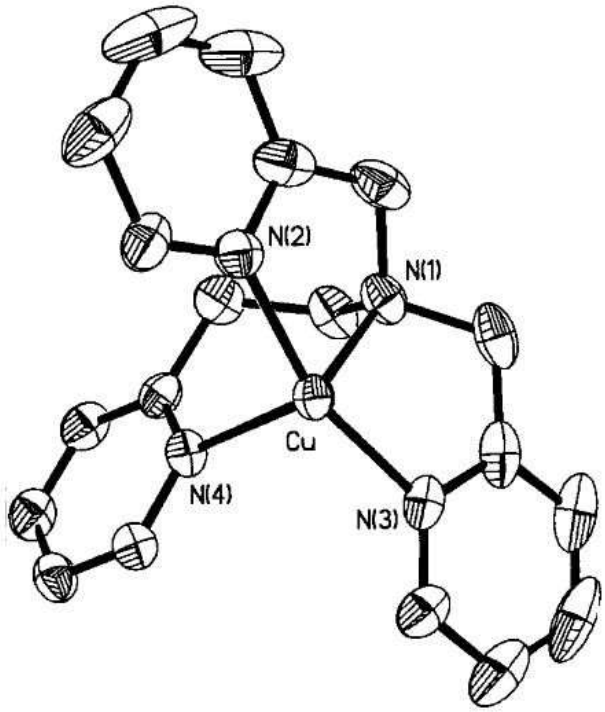


The cyanide anion ($CN^-$, Figure 2) has some interesting bonding properties of its own. It consists of a carbon and nitrogen atom connected by a triple bond and carries an overall molecular charge of negative one. Each atom also has a lone pair of electrons, allowing either side of the molecule to bind metal centers by donating electrons as a Lewis base, making the cyanide anion an effective bridging ligand. Furthermore, it is very compact and capable of not only sigma interactions by direct lone pair donation from the highest occupied molecular orbital (HOMO), but also π-acceptance of electrons into the vacant π*- lowest unoccupied molecular orbital (LUMO, see Figure 3), which is described as π-backbonding.

Figure 2: The Cyanide Anion.

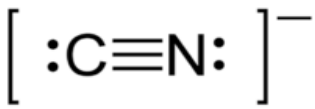

Figure 3: HOMO and LUMO Orbitals for $CN^-$. The cyanide anion, which is analogous to the CO ligand, donates electrons in a sigma sense through the HOMO and accepts electrons in the LUMO through π-backbonding.

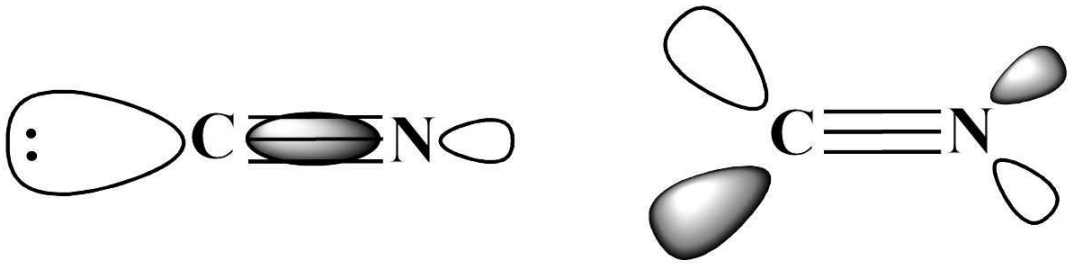

As shown in Figure 4, copper(I) cyanide, CuCN, forms unidimensional polymer chains consisting of two-coordinate metal centers connected by bridging cyano ligands, creating a repeating -X≡X–Cu-X≡X–Cu- sequence, where X is representative of either C or N from the cyanide anion. The sequence of C and N within the chains is random, a condition described as crystallographically disordered.[3] While the high temperature polymorphic form of CuCN is strictly linear, like AgCN and AuCN, the more commonly-studied low temperature form of CuCN shows polymer chains that are slightly wavy. The 2-coordinate nature of CuCN allows for addition of ligands to the polymer structure to form a 3- or 4- coordinate decorated chain without disruption of the CuCN chain. The result is a multitude of ligand interactions to form CuCN-L complexes allowing for a wide range of CuCN:L stoichiometric ratios and structures, an example of which can be seen in Figure 5.

Figure 4: Low Temperature CuCN Chain X-Ray Structure. Representations: Cu atoms, black; disordered C/N atoms, gray.[4]

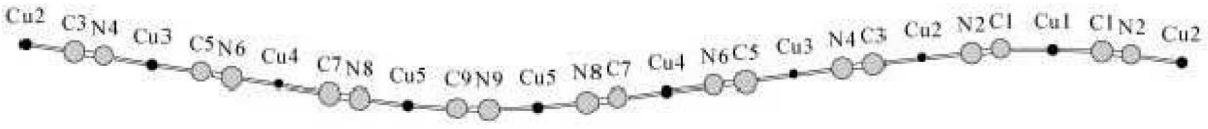

Figure 5: CuCN Chain incorporating 2-methylpyridine Ligand. The addition of 2-methylpyridine creates three-coordinate copper centers without interrupting the CuCN chain structure. Representations: Cu atoms, orange; C atoms, gray; N atoms, blue.[5]

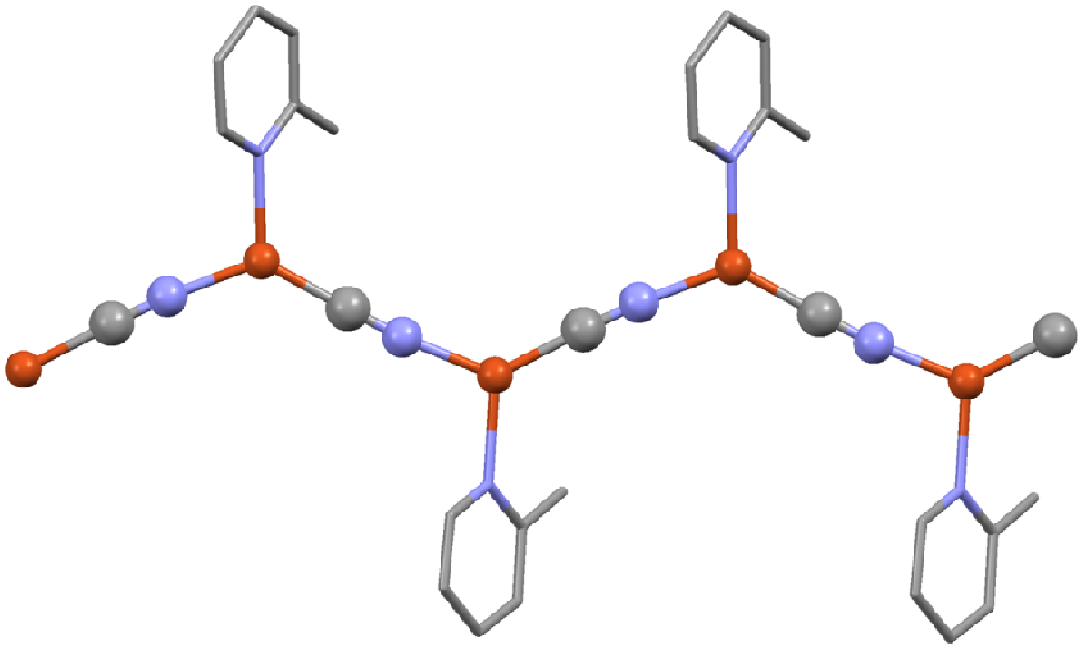

**Luminescent Behavior of Copper(I) Cyanide**

Copper(I) cyanide is a luminescent material with intense emission near the UV/visible border at 392 nm. Coordination of ligands tends to red shift the CuCN emission band well into the visible region. Stevenson and colleagues have looked into the luminescent behavior of aqueous $[Cu(CN)_2]^-$ and were able to conclude that the primary fate of singlet $[Cu(CN)_2]^-$* is electron ejection. However, this competes with intersystem crossing, in which the singlet excited state undergoes an electron spin reversal so that the electrons are no longer spin-paired, producing a triplet state. This excited triplet species is then able to either eject an electron, or react with additional $[Cu(CN)_2]^-$ to form an excited dimer complex, referred to as an excimer.[6]

Possible photophysical causes for luminescence in Cu(I) complexes include metal-to-ligand charge transfer (MLCT), halide-to-ligand charge transfer (XLCT), metal-cluster-centered (CC) transitions, single-metal-centered (MC) transitions, and ligand-centered (LC) transitions. In considering an isolated CuCN chain, XLCT becomes an invalid option since no other halide is present. Cyanide has a very large HOMO-LUMO gap, thus eliminating, LC type transitions. Finally, Cu···Cu distances in CuCN exceed the van der Waals radius sum of 2.8 Å, making CC transitions unlikely (this is not necessarily the case for several CuCN-amine networks, which do contain Cu···Cu distances under 2.8 Å).[7]

Thus, MC and MLCT seem the most likely options for observed luminescence in CuCN, wherein MC transitions are solely dependent on the metal orbitals, while MLCT energy will depend upon the ligand orbitals. A density functional theory (DFT) study by Bayse and Pike comparing CuCN to CuCN–L networks revealed two generalizations: (1) While excitation energy is roughly

the same for CuCN and CuCN-L, CuCN-L emits at lower energy than does CuCN, and (2) CuCN-L networks show distinct high energy (HE) and low energy (LE) emission peaks that can be attributed to MLCT and MC excitations. The study also suggested that excitation spectra arise from intra-strand π–π transitions from occupied to unoccupied π-type molecular orbitals (MOs) (see Figure 6 below), and that the CuCN excitation mechanism is not substantially altered in CuCN-L.

Figure 6: Molecular Orbital (MO) Diagram for $K_2[(Cu(CN_2)]^+$. This diagram shows a molecular orbital transition for a potassium capped CuCN chain with connectivity K–N≡C–Cu–C≡N–K. Transition from the $3\pi_g$ MO (HOMO – 2) to the $4\pi_u$ (LUMO + 2) accounts for the the single band in the excitation spectra. These are the highest occupied and lowest unoccupied π-type MOs.[8]

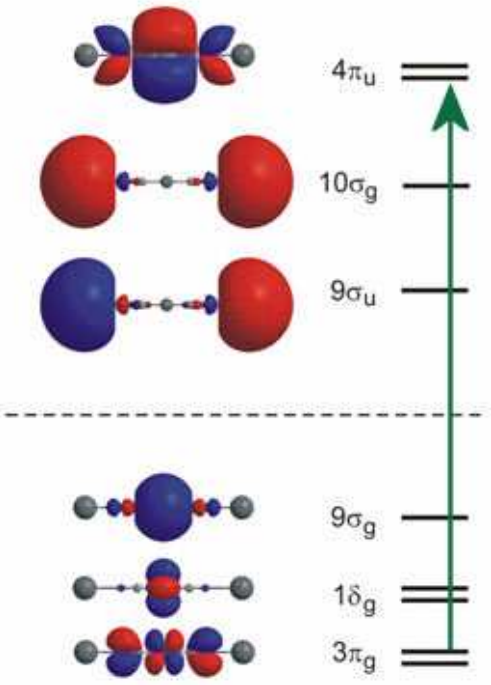

However, luminescence in CuCN and CuCN-L appear to occur by very different processes. The DFT computational results suggested a bent triplet state was responsible for high energy CuCN emissions. Excimer formation, such as those discussed for the $[Cu(CN)_2]^-$ above, would be facilitated by bonding at the bent copper site. Finally, this scenario is consistent with the lower energy luminescence emission seen in lower symmetry three-coordinate CuCN centers, possibly due to lower reorganizational energy associated with triplet formation.[8]

**Development of Luminescent Sensors**

Metal-organic networks have a number of features that make them potentially useful as sensory materials, including chemical reactivity, redox activity, chirality, photoactivity, and, most importantly, porosity. The networks are often constructed in such a way so as to have channels or void space within the network. These spaces allow for the substrate to enter the network, producing a structural change that can result in luminescence or other measurable changes.[9] An example of this behavior is vapochromism, wherein a solid compound will display a change in color when exposed to vapors of a volatile material. Related to this is vapoluminescence, in which a change in luminescence is observed instead of, or in addition to, a change in visible light color.

A good example of a porous system comes from a crystalline, ruthenium-based, oxygen sensor.[10] In the past, luminescent sensory systems based on the $Ru(bpy)_3^{2+}$ (bpy = 2,2'-bipyridine) luminophore have been used to measure dissolved oxygen in aqueous solutions, but this was often complicated by variable amounts of luminescence quenching, as well as decomposition reactions that were initiated by these quenching events. It was discovered that in $[Ru(phen)_3](tfpb)_2$ (phen = 1,10-phenanthroline; tfpb = tetrakis(bis-3,5-trifluoromethylphenylborate)) crystals, the amount of quenching observed is directly related to the amount of void space present in the crystalline cells where oxygen can diffuse into the crystal lattice (See Figure 7). Furthermore, the partially fluorinated counterion $tfpb^-$ was shown to stabilize the degradation of the network such that after one year there were no visible or analytical changes in the crystalline system. After additional testing, it was concluded that $[Ru(phen)_3](tfpb)_2$ served well for detecting gaseous or dissolved oxygen, and that its

symmetrical structure and fluorinated channels helped to eliminate some of the more common problems observed when using these systems.

Figure 7: X-ray Structure of $[Ru(phen)_3](tfpb)_2$ Layers. View down the *b*-axis showing alternating layers of cations and anions. The void space channels (red spheres, 136 $Å^3$ per Ru) run through the cationic layers. Hydrogen atoms omitted for clarity.[10]

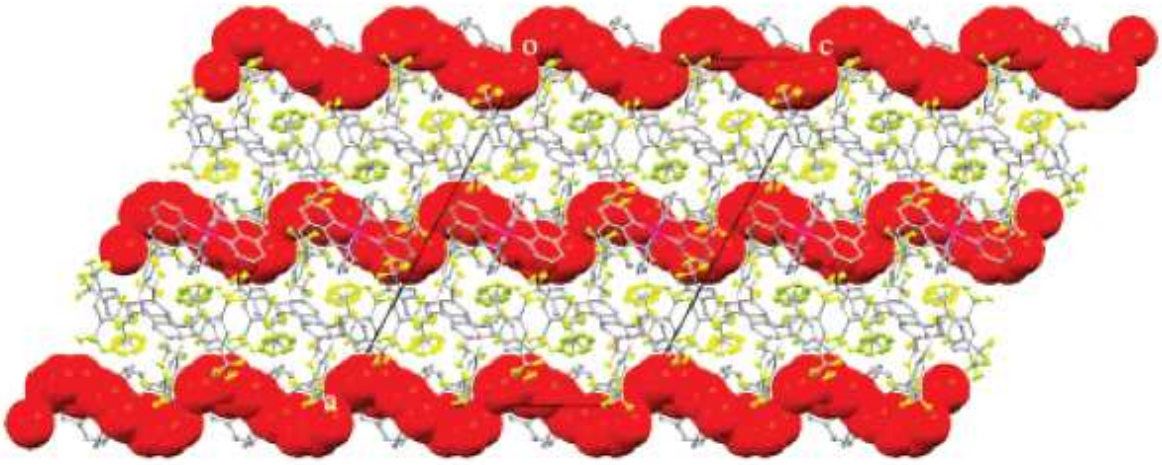

Another interesting VOC sensor is a platinum(II) extended linear chain compound that has been shown to selectively take up benzene. *cis*-Bis(isopropyl isocyanide)dicyanoplatinum(II), $Pt^{II}(CN\text{-}i\text{-}C_3H_7)_2(CN)_2$ ***(IICP)***, forms an extended linear chain (ELC) material that shows a

yellow luminescence under UV excitation. However, when this crystalline film has been exposed to benzene vapors, a change from yellow to blue luminescence occurs, along with a loss of crystallinity. This was studied by isolating $Pt^{II}(CN\text{-}i\text{-}C_3H_7)_2(CN)_2 \bullet 0.5C_6H_6$ (**1BNZ)** from a solution of **(IICP)** in acetonitrile layered in benzene. Following single-crystal studies, the observed results were thought to be a result of a structural change from staggered to eclipsed, which in turn expands the unit cell by 20% in volume, increasing the void space and allowing for the uptake of one benzene for every two **(IICP)** molecules.[11]

Figure 8: Crystal Structure of select Pt (II) Compounds. (a) Single crystal structure for **(IICP)**, view down the *c*-axis. (b)Single-crystal X-ray structure for **(1BNZ)**, view down the *b*-axis. [11]

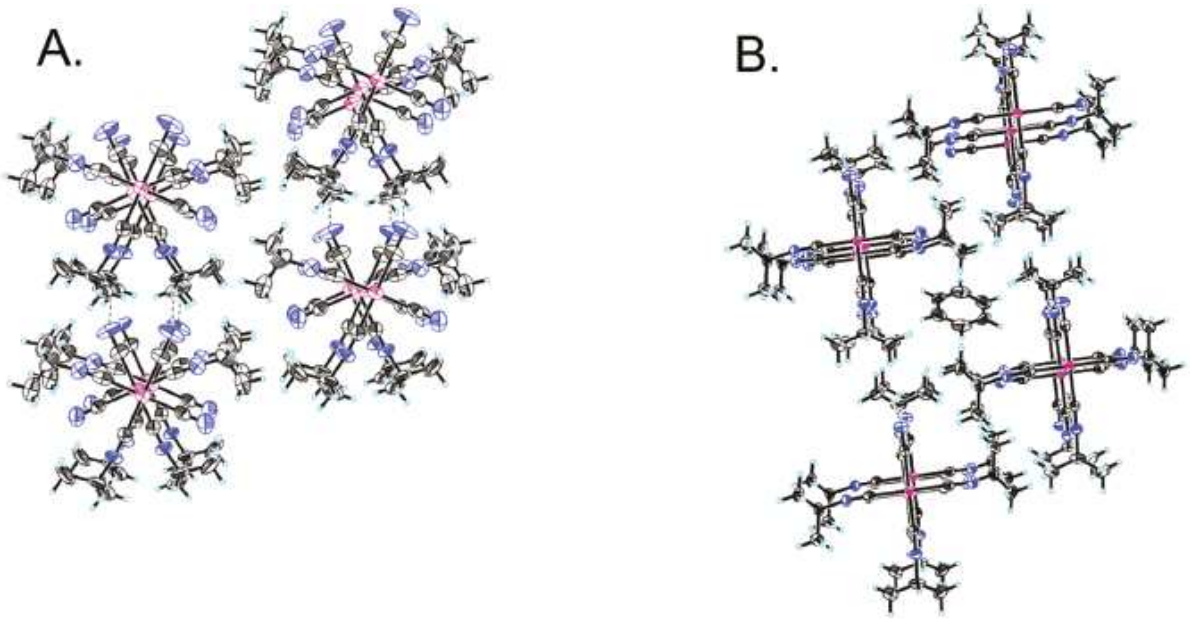

Luminescent studies revealed a shift in maximum emission from 558 to 484 nm after about 20 minutes of exposure to gaseous benzene, confirming the observed visual changes. However several other unique features were discovered during analysis of this compound. Compared to similar structures, **(IICP)** was the only complex to show opening of the crystalline lattice *after* exposure to VOCs instead of utilizing preformed channels, a fact which explains the increase in void space after exposure, however also likely contributes to the relatively lengthy uptake time required to reach equilibrium.

Additionally, the vapor process was shown to be highly selective to benzene; testing with substituted benzene derivatives including toluene, *p*-xylene, *m*-xylene, *o*-xylene, mesitylene, chlorobenzene, and hexafluorobenzene showed no observable luminescent changes. (The reaction with benzene was actually discovered by accident: the chlorobenzene originally used was contaminated with 0.06 M benzene.) While this system is very advantageous as a selective detection system for benzene, other, less desirable characteristics are present. It appears that the crystallinity of the films is key to capturing benzene, and that conversion back to the original benzene-free crystalline form is quite unfavorable due to the large energy change observed in the shift from staggered to eclipsed, as well as substantial changes in volume. As a whole, while the **(IICP)** system showed great selectivity, it was slow to take up benzene, was of low sensitivity, and underwent an irreversible change due to crystalline degradation of the extended linear chain (ELC) material, leaving it far from ideal as a sensor system.[11]

Figure 9: Solid-state luminescence of Pt(II) Crystalline Films. Photograph of **(IICP)** films coating the inside of a cuvette containing (A) air and (B) air saturated with benzene vapor.[11]

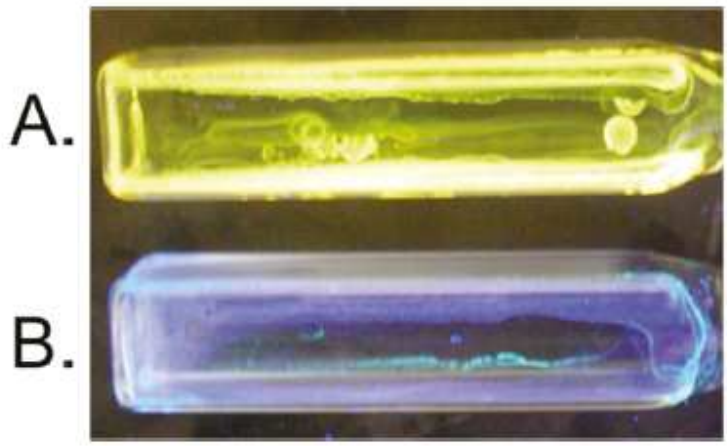


Having examined several properties of copper(I), the cyanide anion, and luminescent properties of CuCN and CuCN-L chains, it is not unreasonable to consider CuCN as a backbone for a metal-organic luminescent sensor for VOCs. When compared to the ruthenium and platinum compounds studied by Dr. Mann, CuCN shows several favorable characteristics. Most important of these is the mechanism of forming an actual VOC-metal complex with low-coordinate Cu(I), rather than simple VOC crystal inclusion. Amine coordination to CuCN results in a luminescence emission shift from the UV into the visible region. The appearance of a new emission signal, rather than enhancement or attenuation of an existing signal, offers a wider dynamic range for sensing applications. The remainder of this thesis will concern investigations of the viability of CuCN as a platform for the detection of amine ligands by luminescence mechanisms.

# EXPERIMENTAL

**Materials and Methods.** All reagents were purchased from Aldrich or Acros and used without purification. All water used was of deionized quality and was thoroughly degassed with Ar.

**General Analyses.** Analyses for C, H, and N were carried out by Atlantic Microlabs, Norcross, GA. Ambient temperature luminescence measurements were carried out on well-ground powders using a Perkin-Elmer LS 55 spectrofluorimeter. Wavelengths were selected with separate excitation and emission monochromators. Solid state quantum yields were measured on the same instrument using a modified version of Mann's method,[10] in which sample comparison is made to a "perfect scatterer", Fluorilon FW-99 (Avian Technologies, Sunapee, NH). IR measurements were made on KBr pellets using a Digilab FTS 7000 FTIR spectrophotometer. Thermogravimetric analyses (TGA) were conducted using a TA Instruments Q500 in the dynamic (variable temp.) mode with a maximum heating rate of 50 $^{o}$C/min. to 300 $^{o}$C under 60 mL/min. $N_2$ flow.

**Atomic Absorption Analysis.** Analyses for Cu were carried out using a Perkin-Elmer AAnalyst 700 atomic absorption instrument. The compounds were prepared by measuring roughly 10–12 mg of the complex in about 1 mL of $HNO_3$, at room temperature, followed by heating the mixture at about 50 $^{o}$C for roughly 10 min. Using ultra-filtered deionized quality water (UFDI), the mixture was transferred to a 100 mL volumetric flask, then diluted a second time to achieve a concentration within calibrated range. Standards were prepared by diluting a 1000 ppm stock solution of

$Cu(NO_3)_2$ to 500, 1000, 1500, 2000, and 2500 ppb in UFDI. Absorption measurements were made at 324 nm.

**X-ray Analysis.** Powder diffraction analysis was carried out on a Bruker *SMART Apex II* diffractometer using graphite-monochromated Cu Kα radiation. Well-ground powder samples were mulled with Paratone N oil. Four frames were collected, covering a 2θ range of 5–100º. The data were processed using *DIFFRAC-Plus* and *EVA* software.

**Tube Reactions.**

Synthesis of $(CuCN)Py_2$, **1a**

Copper(I) cyanide (0.150 g, 1.67 mmol) was suspended in about 5 mL pyridine in a sealed tube under Ar. The mixture was heated to 70 °C in an oil bath overnight without stirring. After cooling, the suspended solid was collected by means of filtration, washed with diethyl ether, and then air dried for 15 min. A yellow powder was isolated (0.393 g, 1.59 mmol, 94.7%). IR ($cm^{-1}$) 2124, 2104, 2086. Anal. Calcd for $C_{11}H_{10}N_3Cu$: C, 53.32; H, 4.07; N, 16.96. Found: C, 52.31; H, 3.96; N, 16.71%. TGA Calcd for (CuCN)Py 68.0. Calcd for $(CuCN)_5Py_4$ 61.7. Found: 68.5 (35–55 °C). Calcd for $(CuCN)_7Py_4$: 54.4. Found: 54.8 (55–80 °C). Calcd for $(CuCN)_3Py$: 46.8. Found: 47.3 (85–110 °C). Calcd for CuCN: 36.1. Found: 36.7 (110–125 °C).

Synthesis of $(CuCN)_5Py_4$, **1b**

The procedure was identical to that used for **1a**, except that the product was vacuum dried overnight. A white powder was isolated (95.3%). IR ($cm^{-1}$) 2126, 2101, 2086. Anal. Calcd for $C_{25}H_{20}N_9Cu_5$: C, 39.29; H, 2.64; N, 16.50. Found: C, 39.37; H, 2.61; N, 16.45%. TGA Calcd for $(CuCN)_7Py_4$: 88.2 Found: 82.8 (55–85 °C). Calcd for $(CuCN)_3Py$: 71.5. Found: 75.8 (85–110 °C). Calcd for CuCN: 58.6. Found: 55.2 (110–130 °C).

Synthesis of $(CuCN)_7Py_4$, **1c**

Complex **1b** (99.0 mg, 0.130 mmol) was suspended in toluene (10 mL) and heated to 70 °C in an oil bath overnight with stirring. A white powder was isolated (82.0 mg, 0.0869 mmol, 93.6%). IR ($cm^{-1}$) 2141, 2136, 2129. Anal. Calcd for $C_{27}H_{20}N_{11}Cu_7$: C, 34.38; H, 2.14; N, 16.33. Found: C, 34.38; H, 1.95; N, 16.19%. TGA Calcd for CuCN: 66.5. Found: 67.0 (95–130 °C).

Synthesis of $(CuCN)_2(2MePy)_3$, **2a**

The procedure was identical to that used for **1a**. A pale yellow powder was isolated (94.5%). IR ($cm^{-1}$) 2128. Anal. Calcd for $C_{20}H_{21}N_5Cu_2$: C, 52.39; H, 4.62; N, 15.27. Found: C, 50.97; H, 4.40; N, 15.23%. TGA Calcd for (CuCN)(2MePy): 79.7. Found 80.9 (35–50 °C). Calcd for $(CuCN)_2(2MePy)$: 59.4. Found 60.3 (50–85 °C). Calcd for CuCN: 39.1. Found 40.3 (85–110 °C).

Synthesis of (CuCN)(2MePy), **2b**

The procedure was identical to that used for **1b**. A white powder was isolated (82.2%). IR ($cm^{-1}$) 2128, 2102. Anal. Calcd for $C_7H_7N_2Cu$: C, 46.02; H, 3.86; N, 15.33. Found: C, 46.02; H, 3.69; N, 15.23%. TGA Calcd for $(CuCN)_2(2MePy)$: 74.5. Found: 77.4 (50– 85 °C). Calcd for CuCN: 49.0. Found: 51.4 (85–110 °C).

Synthesis of $(CuCN)_2(3MePy)_3$, **3a**

The procedure was identical to that used for **1a**. A straw-colored powder was isolated (95.5%). IR ($cm^{-1}$) 2128, 2102. Anal. Calcd for $C_{20}H_{21}N_5Cu_2$: C, 52.39; H, 4.62; N, 15.27. Found: C, 52.37; H, 4.61; N, 14.99%. TGA Calcd for (CuCN)(3MePy): 79.7. Found 75.0 (30–50 °C). Calcd for $(CuCN)_2(3MePy)$: 54.7. Found 56.6 (50–90 °C). Calcd for CuCN: 39.1. Found 36.8 (90–130 °C).

Synthesis of (CuCN)(3MePy), **3b**

The procedure was identical to that used for **1b**. An off-white powder was isolated (81.4%). IR ($cm^{-1}$) 2124, 2112, 2087. Anal. Calcd for $C_7H_7N_2Cu$: C, 46.02; H, 3.86; N, 15.33. Found: C, 45.25; H, 3.79; N, 15.20%. TGA Calcd for $(CuCN)_2(2MePy)$: 74.5. Found: 76.0 (60–100 °C). Calcd for CuCN: 49.0. Found: 50.2 (100–140 °C).

Synthesis of $(CuCN)_2(4MePy)_3$, **4a**

The procedure was identical to that used for **1a**. A pale yellow powder was isolated (100%). IR ($cm^{-1}$) 2115, 2101. Anal. Calc. for $C_{20}H_{21}N_5Cu_2$: C, 52.39; H, 4.62; N, 15.27. Found: C, 52.09; H, 4.58; N, 15.21%. TGA Calcd for (CuCN)(4MePy): 79.7. Found 79.8 (60–85 °C). Calcd for $(CuCN)_2$(4MePy): 54.7. Found 59.5 (85–105 °C). Calcd for CuCN: 39.1. Found 39.3 (105–145 °C).

Synthesis of (CuCN)(2EtPy), **5**

The procedure was identical to that used for **1a**. A white powder was isolated (100%). IR ($cm^{-1}$) 2128. Anal. Calcd for $C_8H_9N_2Cu$: C, 48.85; H, 4.61; N, 14.24. Found: C, 48.65; H, 4.49; N, 14.19%. TGA Calcd for $(CuCN)_2$(2EtPy): 74.5. Found: 77.4 (50–85 °C). Calcd for CuCN: 45.5. Found: 45.9 (65–105 °C).

Synthesis of $(CuCN)_2(3EtPy)_3$, **6a**

The procedure was similar to that used for **1a**. In this case a solution was quickly formed in the 3EtPy. Once the solution had formed (30 min.), the mixture was cooled, causing spontaneous crystallization of the product. A pale yellow powder was isolated (94.4%). IR ($cm^{-1}$) 2119, 2106. Anal. Calc. for $C_{23}H_{27}N_5Cu_2$: C, 55.19; H, 5.44; N, 13.99. Found: C, 55.08; H, 5.44; N, 13.97%. TGA Calcd for $(CuCN)_2$(3EtPy): 57.2. Found 58.9 (45–105 °C). Calcd for $(CuCN)_4$(3EtPy): 46.5. Found 48.7 (105–240 °C). Calcd for CuCN: 35.8. Found 37.7 (240–300 °C).

Synthesis of (CuCN)(3EtPy), **6b**

The procedure was identical to that used for **1b**. A white powder was isolated (99.5%). IR ($cm^{-1}$) 2125, 2107. Anal. Calcd for $C_8H_9N_2Cu$: C, 48.85; H, 4.61; N, 14.24. Found: C, 49.06; H, 4.66; N, 13.95%. TGA Calcd for CuCN: 45.5. Found: 47.5 (90–125 °C).

Synthesis of (CuCN)(4EtPy), **7**

The procedure was identical to that used for **1a**. In this case a solution was formed in the 4EtPy. Addition of $Et_2O$ was required to precipitate the product. A tan powder was isolated (77.4%). IR ($cm^{-1}$) 2130, 2123. Anal. Calcd for $C_8H_9N_2Cu$: C, 48.85; H, 4.61; N, 14.24. Found: C, 48.03; H, 4.47; N, 14.08%. TGA Calcd for $(CuCN)_4(4EtPy)_3$: 86.4. Found 86.2 (60–110 °C). Calcd for $(CuCN)_4$(4Et-Py): 59.1. Found 62.0 (110–150 °C). Calcd for CuCN: 45.5. Found 47.5 (150–300 °C).

Synthesis of (CuCN)(2ClPy), **8a**

The procedure was identical to that used for **1a**. A yellow powder was isolated (84.1%). IR ($cm^{-1}$) 2129. Anal. Calcd for $C_6H_4N_2ClCu$: C, 35.48; H, 1.99; N, 13.79. Found: C, 35.27; H, 1.89; N, 13.92%. TGA Calcd for CuCN: 44.1. Found 46.6 (50–80 °C).

Synthesis of (CuCN)(3ClPy), **9a**

The procedure was identical to that used for **1a**. An off-white powder was isolated (90.8%). IR ($cm^{-1}$) 2139, 2117, 2100, 2088. Anal. Calcd for $C_6H_4N_2ClCu$: C, 35.48; H, 1.99; N, 13.79. Found: C, 35.31; H, 1.88; N, 13.75%. TGA Calcd for $(CuCN)_2(3ClPy)$: 72.0. Found 72.1. (60–90 °C). Calcd for CuCN: 44.1. Found 44.5 (90–120 °C).

Synthesis of (CuCN)(2BrPy), **10a**

The procedure was identical to that used for **1a**. An off-white powder was isolated (91.1%). IR ($cm^{-1}$) 2128. Anal. Calc. for $C_6H_4N_2BrCu$: C, 29.11; H, 1.63; N, 11.32. Found: C, 28.11; H, 1.44; N, 11.53%. TGA Calcd for $(CuCN)_4(2BrPy)_3$: 84.0. Found 84.7 (30–65 °C). Calcd for CuCN: 36.2. Found 38.7 (65–115 °C).

Synthesis of (CuCN)(3BrPy), **11**

The procedure was identical to that used for **1a**. A white powder was isolated (95.3%). IR ($cm^{-1}$) 2126, 2112, 2100. Anal. Calcd for $C_6H_4N_2BrCu$: C, 29.11; H, 1.63; N, 11.32. Found: C, 29.18; H, 1.53; N, 11.36%. TGA Calcd for $(CuCN)_2(3BrPy)$: 68.0. Found 69.3 (85–105 °C). Calcd for CuCN: 36.2. Found 37.4 (105–130 °C).

Synthesis of $(CuCN)(3MeOPy)_2$, **12**

The procedure was identical to that used for **1a**. An off-white powder was isolated (91.5%). IR ($cm^{-1}$) 2098, 2083. Anal. Calcd for $C_{13}H_{16}N_3O_2Cu$: C, 50.40; H, 5.21; N, 13.56. Found: C, 50.49; H, 4.64; N, 13.64%. TGA Calcd for (CuCN)(3MeOPy): 64.5. Found 66.8 (50–80 °C). Calcd for $(CuCN)_3(3MeOPy)_2$: 52.7. Found 54.4 (80–105 °C). Calcd for CuCN: 29.1. Found 30.3 (105–130 °C).

Synthesis of $(CuCN)_2(4^tBuPy)_3$, **13a**

The procedure was identical to that used for **1a**. A yellow crystalline solid was isolated (94.7%). IR ($cm^{-1}$) 2124. Anal. Calcd for $C_{23}H_{27}N_5Cu_2$: C, 55.19; H, 5.44; N, 13.99. Found: C, 55.08; H, 5.44; N, 13.97%. TGA Calcd for $(CuCN)_2(4^tBuPy)$: 57.2. Found 58.9 (45–105 °C). Calcd for $(CuCN)_4(4^tBuPy)$: 46.5. Found 48.7 (105–240 °C). Calcd for CuCN: 35.8. Found 34.5 (240–15 °C).

Synthesis of (CuCN)(26Lut), **14**

The procedure was identical to that used for **1a**. A white powder was isolated (98.0%). IR ($cm^{-1}$) 2128. Anal. Calcd for $C_8H_9N_2Cu$: C, 48.85; H, 4.61; N, 14.21. Found: C, 48.56; H, 4.41; N, 14.03%. TGA Calcd for CuCN: 45.5. Found 45.7 (85–125 °C).

Synthesis of (CuCN)(246Coll), **15**

The procedure used for **1a** did not effect complete conversion. Exchange reaction: 247 mg (0.323 mmol) **1b** was suspended in about 5 mL 246Coll in a sealed tube under Ar. The mixture was heated to 70 °C in an oil bath overnight without stirring. After cooling, the suspended solid was collected by means of filtration, washed with diethyl ether, and then air dried. A white powder was isolated (0.318 g, 2.86 mmol, 88.4%). IR ($cm^{-1}$) 2162, 2125. Anal. Calcd for $C_9H_{11}N_2Cu$: C, 51.29; H, 5.26; N, 13.29. Found: C, 51.02; H, 5.24; N, 13.36%. TGA Calcd for CuCN: 42.5. Found 42.9 (85–145 °C).

Synthesis of (CuCN)(Quin), **16**

The exchange procedure was identical to that used for **15**. A white powder was isolated (90.0%). IR ($cm^{-1}$) 2123. Anal. Calcd for $C_{10}H_7N_2Cu$: C, 54.91; H, 3.23; N, 12.81. Found: C, 54.61; H, 3.07; N, 12.81%. TGA Calcd for CuCN: 40.9. Found 41.4 (135–175 °C).

Synthesis of (CuCN)($NEt_3$), **17a**

The procedure was identical to that used for **1a**. A white powder was isolated (92.6%). IR ($cm^{-1}$) 2129. Anal. Calcd for $C_7H_{15}N_2Cu$: C, 44.08; H, 7.93; N, 14.69. Found: C, 42.25; H, 7.48; N, 14.66%. TGA Calcd for $(CuCN)_2(NEt_3)$: 73.5. Found 65.9 (35–55 °C). Calcd for CuCN: 46.9. Found 48.3 (55–75 °C).

Synthesis of $(CuCN)(NHEt_2)$, **18**

The procedure was identical to that used for **1a**. An off-white powder was isolated (90.6%). IR ($cm^{-1}$) 2120, 2116. Anal. Calcd for $C_7H_{15}N_2Cu$: C, 36.91; H, 6.81; N, 17.22. Found: C, 36.62; H, 6.73; N, 17.09%. TGA Calcd for CuCN: 55.0. Found 55.8 (50–75 °C).

Synthesis of $(CuCN)_2(NH^iPr_2)$, **19**

The procedure was identical to that used for **1a**. A straw-colored powder was isolated (92.3%). IR ($cm^{-1}$) 2158, 2135. Anal. Calcd for $C_8H_{15}N_3Cu_2$: C, 34.28; H, 5.39; N, 14.99. Found: C, 36.70; H, 5.80; N, 14.62%. TGA Calcd for CuCN: 63.9. Found 63.6 (40–85 °C).

Synthesis of $(CuCN)_3(Pipd)_4$, **20a**

The procedure was identical to that used for **1a**. In this case a solution was formed in the Pipd. Upon cooling a white powder was isolated (97.6%). IR ($cm^{-1}$) 2120, 2105, 2072. Anal. Calcd for $C_{18}H_{44}N_7Cu_3$: C, 45.34; H, 7.28; N, 16.09. Found: C, 44.61; H, 7.16; N, 15.97%. TGA Calcd for $(CuCN)_3(Pipd)_2$: 72.0. Found 75.0 (35–90 °C). Calcd for $(CuCN)_3(Pipd)$: 58.1. Found 58.8 (90–215 °C). Calcd for CuCN: 44.1. Found 44.5 (215–270 °C).

Synthesis of (CuCN)(MePipd), **21a**

The procedure was identical to that used for **1a**. A pale yellow powder was isolated (99.3%). IR ($cm^{-1}$) 2139, 2132. Anal. Calcd for $C_7H_{13}N_2Cu$: C, 44.55; H, 6.94; N, 14.84. Found: C, 43.83; H, 6.85; N, 14.99%. TGA Calcd for $(CuCN)_2$(MePipd): 73.7. Found 70.2 (45–70 °C). Calcd for CuCN: 47.5. Found 49.5 (70–100 °C).

Synthesis of $(CuCN)_4(EtPipd)_3$, **22**

The procedure was identical to that used for **1a**. An off-white powder was isolated (97.5%). IR ($cm^{-1}$) 2128. Anal. Calcd for $C_{25}H_{45}N_7Cu_4$: C, 43.03; H, 6.50; N, 14.05. Found: C, 43.14; H, 6.55; N, 13.91%. TGA Calcd for $(CuCN)_4$(Pipd): 67.6. Found 68.0 (55–90 °C). Calcd for CuCN: 51.3. Found 50.3 (90–105 °C).

Synthesis of (CuCN)(MePyrrolid), **23**

The procedure was identical to that used for **1a**. A white powder was isolated (93.3%). IR ($cm^{-1}$) 2130. Anal. Calcd for $C_6H_{11}N_2Cu$: C, 41.25; H, 6.35; N, 16.03. Found: C, 40.38; H, 6.20; N, 15.91%. TGA Calcd for $(CuCN)_2$(MePyrrolid): 75.6. Found 72.0 (35–75 °C). Calcd for CuCN: 51.3. Found 51.8 (75–105 °C).

Synthesis of $(CuCN)_2(Morph)_3$, **24a**

The procedure was identical to that used for **1a**. A white powder was isolated (93.8%). IR ($cm^{-1}$) 2126. Anal. Calcd for $C_{14}H_{27}N_5O_3Cu_2$: C, 38.17; H, 6.18; N, 15.90. Found: C, 37.45; H, 6.10; N, 15.81%. TGA Calcd for (CuCN)(Morph): 80.2. Found 78.4 (50–70 °C). Calcd for $(CuCN)_3$(Morph): 53.9. Found 52.8 (70–105 °C). Calcd for CuCN: 40.7. Found 40.1 (105–135 °C).

Synthesis of (CuCN)(Morph), **24b**

The procedure was identical to that used for **1b**. A pale yellow powder was isolated (100%). IR ($cm^{-1}$) 2126. Anal. Calcd for $C_5H_9N_2OCu$: C, 33.99; H, 5.13; N, 15.85. Found: C, 34.23; H, 5.17; N, 15.74%. TGA Calcd for $(CuCN)_3$(Morph): 67.1. Found 67.6 (55–105 °C). Calcd for CuCN: 50.7. Found 51.1 (105–130 °C).

Synthesis of (CuCN)(MeMorph), **25a**

The procedure was identical to that used for **1b**. A pale yellow powder was isolated (94.2%). IR ($cm^{-1}$) 2120. Anal. Calcd for $C_6H_{11}N_2OCu$: C, 37.79; H, 5.81; N, 14.69. Found: C, 37.02; H, 5.73%; N, 14.67. TGA Calcd for $(CuCN)_3$(MeMorph): 64.6. Found 63.3 (55–95 °C). Calcd for CuCN: 47.0. Found 47.3 (95–140 °C).

Synthesis of (CuCN)($NMe_2Cy$), **26a**

The procedure was identical to that used for **1a**. An off-white crystalline solid was isolated (93.7%). IR ($cm^{-1}$) 2073. Anal. Calcd for $C_9H_{17}N_2Cu$: C, 49.86; H, 7.90; N, 12.92. Found: C, 49.96; H, 7.99; N, 12.76%. TGA Calcd for $(CuCN)_3(NMe_2Cy)$: 60.9. Found 62.3 (45–80 °C). Calcd for CuCN: 42.2. Found 42.2 (75–110 °C).

Synthesis of $(CuCN)(1MeIm)_3$, **27**

The procedure was identical to that used for **1a**. A white crystalline solid was isolated (93.0%). IR ($cm^{-1}$) 2137. Anal. Calcd for $C_{13}H_{18}N_7Cu$: C, 46.49; H, 5.40; N, 29.19. Found: C, 46.72; H, 5.33; N, 29.34%. TGA Calcd for $(CuCN)_2(1MeIm)_3$: 63.3. Found 59.0 (55–90 °C). Calcd for $(CuCN)_2(1MeIm)$: 38.9. Found 36.9 (90–205 °C). Calcd for CuCN: 26.7. Found 32.5 (205–285 °C).

Synthesis of $(CuCN)_3(Me_2S)$, **28**

The procedure was identical to that used for **1a**. A white crystalline solid was isolated (84.1%). IR ($cm^{-1}$) 2145, 2125. Anal. Calcd for $C_5H_6N_3SCu_3$: C, 18.15; H, 1.83; N, 12.70. Found: C, 18.08; H, 1.65; N, 12.71%. TGA Calcd for $(CuCN)_9(Me_2S)$: 87.5. Found 87.6 (30–55 °C). Calcd for CuCN: 81.2. Found 80.5 (55–105 °C).

Synthesis of (CuCN)(THT), **29**

The exchange procedure was identical to that used for **15**. A white crystalline solid was isolated (70.4%). IR ($cm^{-1}$) 2122. Anal. Calcd for $C_5H_8NSCu$: C, 33.79; H, 4.54; N, 7.88. Found: C, 33.32; H, 4.31; N, 7.88%. TGA Calcd for CuCN: 50.4. Found 50.7 (65–125 °C).

**Vial Reactions**

Synthesis of $(CuCN)_2(Py)_3$, **30**

Copper(I) cyanide (0.180 g, 2.00 mmol) was suspended in about 2 mL pyridine in a sealed vial under Ar. The mixture was allowed to stir for three days at room temperature, collected by means of filtration, washed with diethyl ether, and then air dried for 15 min. A pale yellow powder was isolated (83.3%). Anal. Calcd for $C_{17}H_{15}N_5Cu_2$: C, 49.03; H, 3.60; N, 16.82. Found: C, 47.68; H, 3.50; N, 16.54. TGA Calcd (CuCN)(Py): 81.0. Found 78.3 (40–50°C). Calcd for $(CuCN)_2(Py)$: 62.0. Found 61.8 (50–80°C). Calcd for $(CuCN)_4(Py)$: 52.5. Found 51.2 (80–106). Calcd for CuCN: 43.0. Found 42.2 (115–112 °C).

Synthesis of $(CuCN)_x(2MePy)_y$, **31**

The procedure was identical to that used for **30**. A white powder was isolated**.** TGA Found for CuCN 43.12 (80–100 °C). Anal. Found: C, 44.42; H, 4.01; N, 15.68. AAS Found for Cu: 32.2.

Synthesis of $(CuCN)_3(3MePy)_2$, **32**

The procedure was identical to that used for **30**. A tan brown powder was isolated (88.1%). TGA Calcd for $(CuCN)_3(3MePy)$: 79.7. Found 77.5 (50–80°C). Calcd for CuCN: 59.3. Found 56.0 (80–135 °C).

Synthesis of $(CuCN)_2(4MePy)_3$, **33**

The procedure was identical to that used for **30**. A white powder was isolated (92.8%). Anal. Calcd for $C_{20}H_{21}N_5Cu_2$: C, 52.34; H, 4.58; N, 15.27. Found: C, 52.17; H, 4.42; N, 14.83. TGA Calcd for (CuCN)(4MePy): 79.7. Found 80.6 (50–85 °C). Calcd for $(CuCN)_2(4MePy)$: 59.3. Found 60.8 (95–105°C). Calcd for CuCN: 39.0. Found 40.7 (105–145 °C).

Synthesis of (CuCN)(2EtPy), **34**

The procedure was identical to that used for **30**. A white powder was isolated (92.4%). TGA Calcd for CuCN: 45.5. Found 46.5 (75–105 °C).

Synthesis of (CuCN)(3EtPy), **35**

The procedure was identical to that used for **30**. A white powder was isolated (118.6%). TGA Calcd for $(CuCN)_2(2EtPy)$: 72.8. Found 72.5 (50–120 °C). Calcd for CuCN: 45.5. Found 44.3 (117–270 °C).

Synthesis of $(CuCN)_3(2ClPy)_2$, **36**

The procedure was identical to that used for **30**. A white powder was isolated (61.3%). TGA Calcd for CuCN: 54.2. Found 56.9 (60–84 °C).

Synthesis of (CuCN)(3ClPy), **37**

The procedure was identical to that used for **30**. A yellow powder was isolated (53.6%). TGA Calcd for $(CuCN)_2(3ClPy)$: 72.0. Found 68.0 (50–80 °C). Calcd for CuCN: 44.1. Found 42.6 (80–120 °C).

Synthesis of (CuCN)(2BrPy), **38**

The procedure was identical to that used for **30**. A white powder was isolated (68.7%). TGA Calcd for $(CuCN)_2(2BrPy)$: 68.0 Found 64.3 (50–95 °C). Calcd for CuCN: 36.2. Found 38.8 (95–135 °C).

Synthesis of (CuCN)(3BrPy), **39**

The procedure was identical to that used for **30**. A yellow powder was isolated (111.6%). Anal. Calc. for $C_6H_4N_2Cu$: C, 29.08; H, 1.62; N, 11.31. Found: C, 29.95; H, 1.73; N, 10.19. AAS Calcd for Cu: 25.7. Found 24.3. TGA Calcd for CuCN: 39.0. Found 48.3 (80–110 °C).

2.32. Synthesis of (CuCN)(26Lut), **40**

The procedure was identical to that used for **30**. A white powder was isolated (88.0%). TGA Calcd for CuCN: 45.5. Found 46.0 (95–120 °C).

Synthesis of (CuCN)(246Coll), **41**

The procedure was identical to that used for **30**. A white powder was isolated (91.5%) TGA Calcd for CuCN: 42.5. Found 45.7 (110–140 °C).

Synthesis of (CuCN)(Quin), **42**

The procedure was identical to that used for **30**. A white powder was isolated (95.1%) TGA Calcd for CuCN: 40.9. Found 41.2 (140–165 °C).

Synthesis of $(CuCN)_3(NEt_3)$, **43**

The procedure was identical to that used for **30**. A brown powder was isolated (88.5%). Anal. Calcd for $C_9H_{15}N_4Cu_3$: C, 29.22; H, 4.06; N, 15.15. Found: C, 30.89; H, 4.36; N, 14.67. AAS Calcd for Cu: 51.6. Found 51.4. TGA Calcd for CuCN: 72.6. Found 76.0 (50–85 °C).

Synthesis of $(CuCN)(NHEt_2)$, **44**

The procedure was identical to that used for **30**. A white powder was isolated (95.1%). TGA Calcd for CuCN: 55.0. Found 56.7 (60–75 °C).

Synthesis of (CuCN)(Pipd), **45**

The procedure was identical to that used for **30**. A brown powder was isolated (95.3%). AAS Calcd for Cu: 36.4. Found 37.7. TGA Calcd for $(CuCN)_2$(Pipd): 75.6. Found 77.9 (112–217 °C). Calcd for $(CuCN)_4$(Pipd): 63.4. Found 63.8 (217–342 °C). Calcd for CuCN: 51.3. Found 50.1 (347–370 °C).

Synthesis of $(CuCN)_3(MePipd)_2$, **46**

The procedure was identical to that used for **30**. A yellow powder was isolated (93.2%). Anal. Calcd for $C_{15}H_{26}N_5Cu_3$: C, 38.54; H, 5.57; N, 14.99. Found: C, 39.13; H, 5.70; N, 14.01. TGA Calcd for $(CuCN)_3$(MePipd): 78.8. Found 80.6 (50–65 °C). Calcd for CuCN: 57.5. Found 57.0 (65–100 °C).

Synthesis of $(CuCN)_4(EtPipd)_3$, **47**

The procedure was identical to that used for **30**. A white powder was isolated (95.4%). TGA Calcd for $(CuCN)_2$(EtPipd): 83.8. Found 82.2 (55–65°C). Calcd for CuCN: 51.3. Found 50.9 (65–100 °C).

Synthesis of (CuCN)(MePyrrolid), **48**

The procedure was identical to that used for **30**. A brown powder was isolated (110.9%). Anal. Calcd for $C_{16}H_{11}N_2$ Cu: C, 41.25; H, 6.35; N, 16.04. Found: C, 39.64; H, 6.07; N, 15.27. TGA Calcd for $(CuCN)_2$(MePyrrolid): 75.6. Found 81.7 (55–80 °C). Calcd for CuCN: 51.3. Found 57.6 (80–135 °C).

Synthesis of $(CuCN)_2(Morph)_3$, **49**

The procedure was identical to that used for **30**. A white powder was isolated (99.3%) TGA Calcd for $(CuCN)_4(Morph)_3$: 70.3. Found 70.8 (60–75 °C). Calcd for $(CuCN)_4$(Morph): 50.6. Found 47.6 (75–115 °C). Calcd for CuCN: 34.0. Found 37.1 (115–140 °C).

Synthesis of (CuCN)(MeMorph), **50**

The procedure was identical to that used for **30**. A green powder was isolated (75.2%). TGA Calcd for $(CuCN)_3$(MeMorph): 64.6. Found 64.2 (75–90 °C). Calcd for CuCN: 47.0 Found 48.9 (90–140 °C).

Synthesis of $(CuCN)_3(NMe_2Cy)$, **51**

The procedure was identical to that used for **30**. A green powder was isolated (80.4%) TGA Calcd for CuCN: 67.7. Found 66.8 (75–115 °C).

**General Method for Exchange Reactions**

Copper(I) cyanide (0.150 g, 1.67 mmol) was suspended in about 5 mL of a ligand (L) in a sealed tube under Ar. The mixture was heated to 70 °C in an oil bath overnight without stirring. After cooling, the suspended solid was collected by means of filtration, washed with diethyl ether, and then air dried for 15 min. This product was then suspended in about 5 mL of a second ligand (L') in a sealed tube under Ar and heated to 70 °C in an oil bath overnight without stirring. After cooling, the suspended solid was collected by means of filtration, washed with diethyl ether, and then air dried for 15 min.

**General Method for Liquid-Exposed Samples**

A few drops of liquid amine were directly added to CuCN powder, which was then ground in a mortar and pestle to promote homogeneity.

**Formation of CuCN Pellets**

Copper(I) cyanide powder (0.089 g, 1.00 mmol) was sealed inside the center of an IR pellet press that had been lubricated with white vacuum grease. Torque was applied to the outer screws to press the powder into a pellet, which was then removed from the bolt with a precision knife.

**General Method for Vapor Diffused Pellet Samples**

A copper(I) cyanide pellet prepared as described above was attached to the bottom of a 2-dram vial using double-sided tape. The 2-dram vial was then inserted upside-down into a larger jar containing 2−3 mL of liquid amine. The jar was then capped and allowed to sit overnight before the inner vial was removed to isolate the resulting product.

**Formation of CuCN Impregnated Polymer Films**

50 mL of tetrahydrofuran (47.0 g, 0.65mol) was heated on a hotplate to 40 °C with vigorous stirring. To this, 8.0 g of polyvinylchloride (PVC) was added slowly until completely dissolved to form a 15% by weight stock solution. 10 mL of the PVC stock solution was transferred to a

beaker and stirred vigorously on a hotplate at 40 °C. Copper(I) cyanide (0, 2.0, 4.0, 6.0, or 8.0 g) was then suspended in this solution to form various ratios by weight. The resulting suspension was poured onto a glass plate and pulled to a thickness of 0.381 mm by placing a doctor blade on the plate above the suspension and pulling it down to the bottom of the plate. The suspension was then left to dry overnight and collected the next day using a small razor blade to peel up the edges of the dried film.

# RESULTS AND DISCUSSION

Past research in the Pike research group has focused on the characterization of basic amine interactions with copper(I) cyanide and the luminescence that results from these interactions. In the current work, we wished to delve deeper into the CuCN-amine system and developed experiments to investigate alternative synthetic methods for these compounds in the hopes of discovering a route to the final goal of sensory device fabrication. The methods we used included heated neat amine exchange reactions, room temperature neat amine addition reactions, CuCN pellet amine exposure reactions, and CuCN-impregnated polymer film synthesis. Furthermore, additional research was done to explore in more detail the properties of certain CuCN-amine compounds, including their thermodynamic domains, kinetics of formation, and luminescence quantum yield.

## Tube Reaction Products

In the previous work in our lab, 'authentic' CuCN-amine products were synthesized by suspending CuCN in neat liquid amine in a thick-walled pressure tube under argon gas and heating at 70 °C in an oil bath for a period of about sixteen hours. Both aromatic and aliphatic amines and aromatic imines were used in this method, forming products that were, for the most part, highly luminescent. A complete list of relevant ligands is shown in Figure 10 below and is followed by a photograph showing the resulting luminescence behavior in Figure 11, which

displays several product samples in a well plate under ultraviolet light at 254 and 365 nm. Powders were the most common products and were typically white under visible light, however crystals were also occasionally collected.

Figure 10: Complete List of Ligands (L) Used to Create Tube Reaction Products. See Table 1 for interpretation of abbreviations.[12]

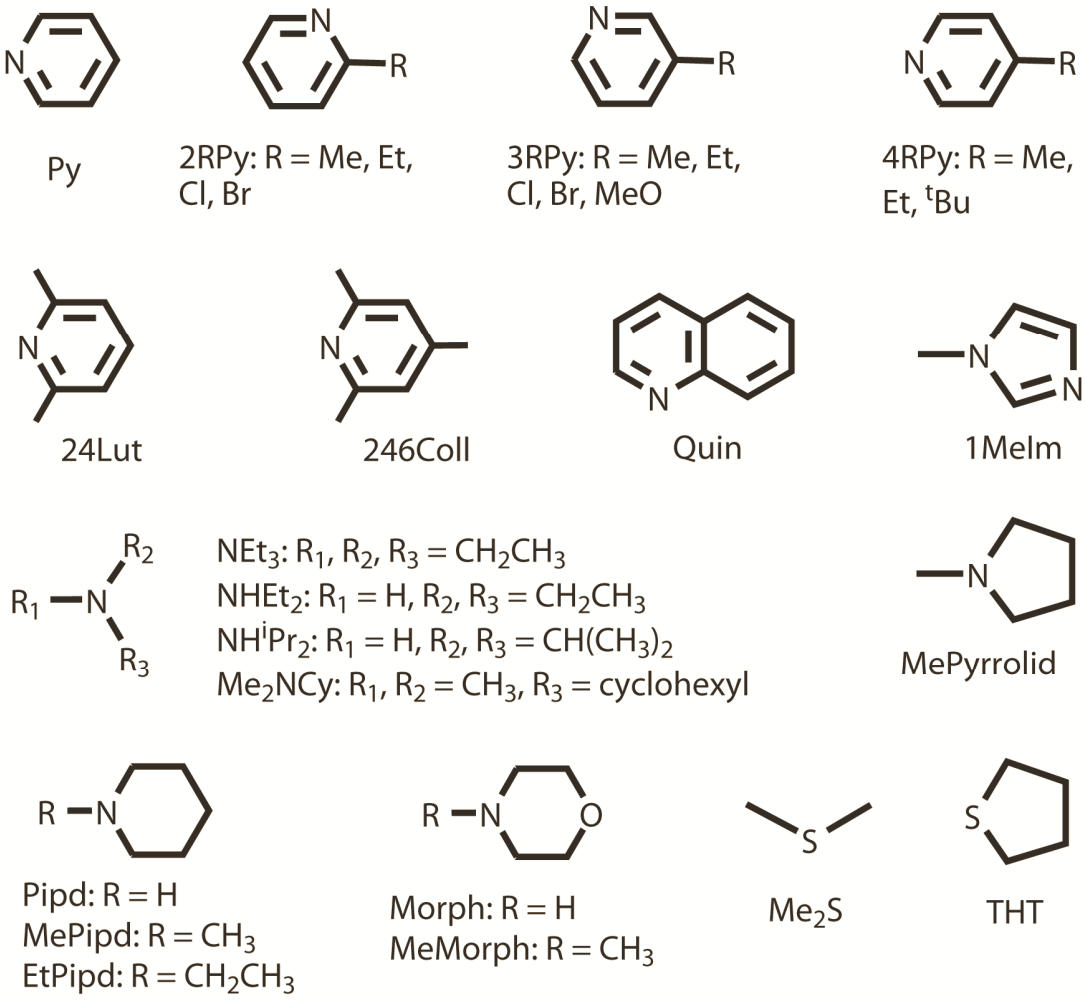

Figure 11: Photograph of $(CuCN)L_n$ Complexes Formed by the Tube Reaction Method. Photograph taken under 254 and 365 nm UV light. See Table 1 for interpretation of compound codes.[12]

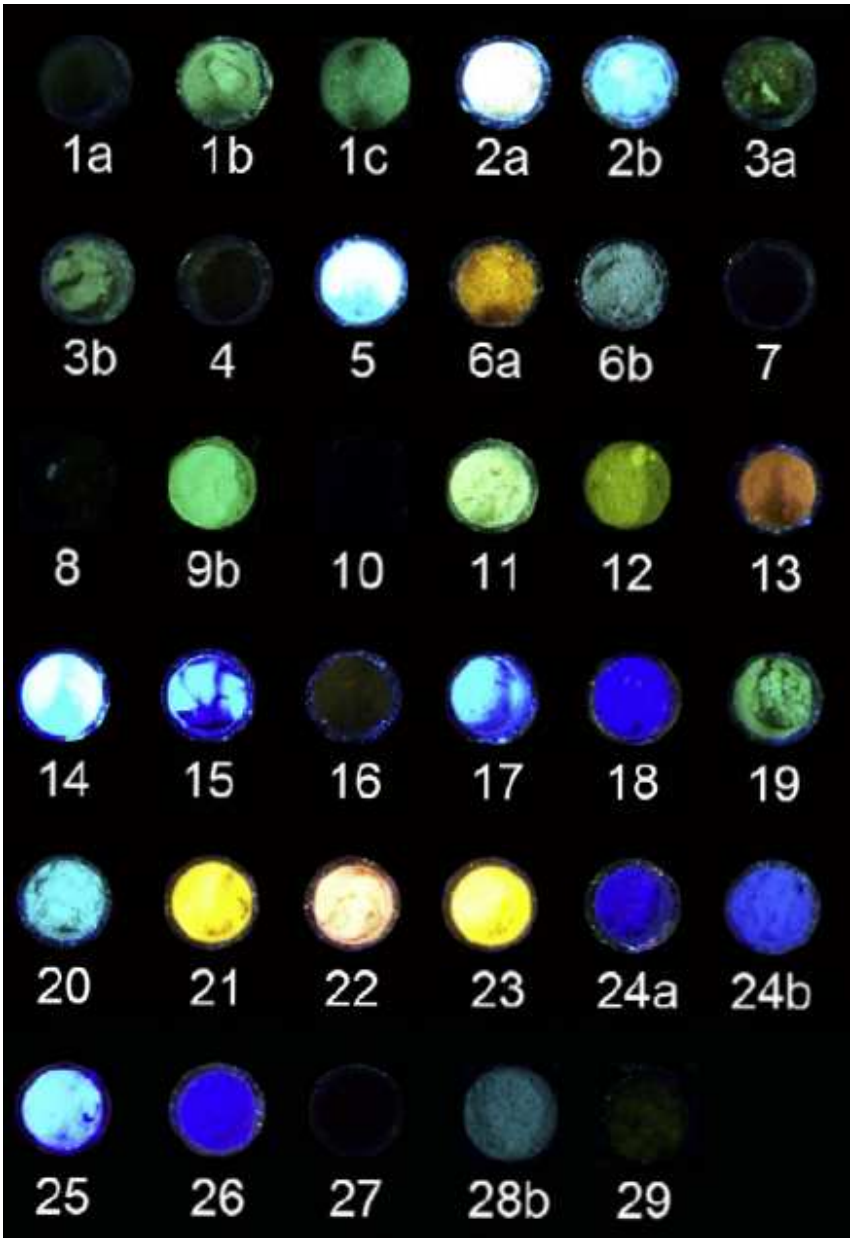

We also examined surface adducts formed by adding drops of liquid L to CuCN powder under 254 nm excitation, shown in Figure 12. By comparison, there is much similarity in the luminescent behavior observed between the two methods. Most noteworthy is the fact that these products display a wide range of emission colors, especially when comparing chemically similar amines, such as the various substituted pyridines (Py) or piperidines (Pipd). These observations are significant in showing that there is a potential use for CuCN as a volatile organic compound (VOC) sensor, as exposure to amines shifts CuCN emission centered at 392 nm well into the visible region.

Figure 12: Luminescence of CuCN + Liquid L Under 254 nm Light at Room Temperature. A: Pipd, B: MePipd, C: EtPipd, D: MePyrrolid, E: $Me_2NCy$, F: $NEt_3$, G: MeMorph, H: MePip, I: $Me_2Pip$, J: Py, K: 2MePy, L: 3MePy, M: 4MePy, N: 2EtPy, O: 3EtPy, P: 4EtPy, Q: 4$^t$BuPy.[5]

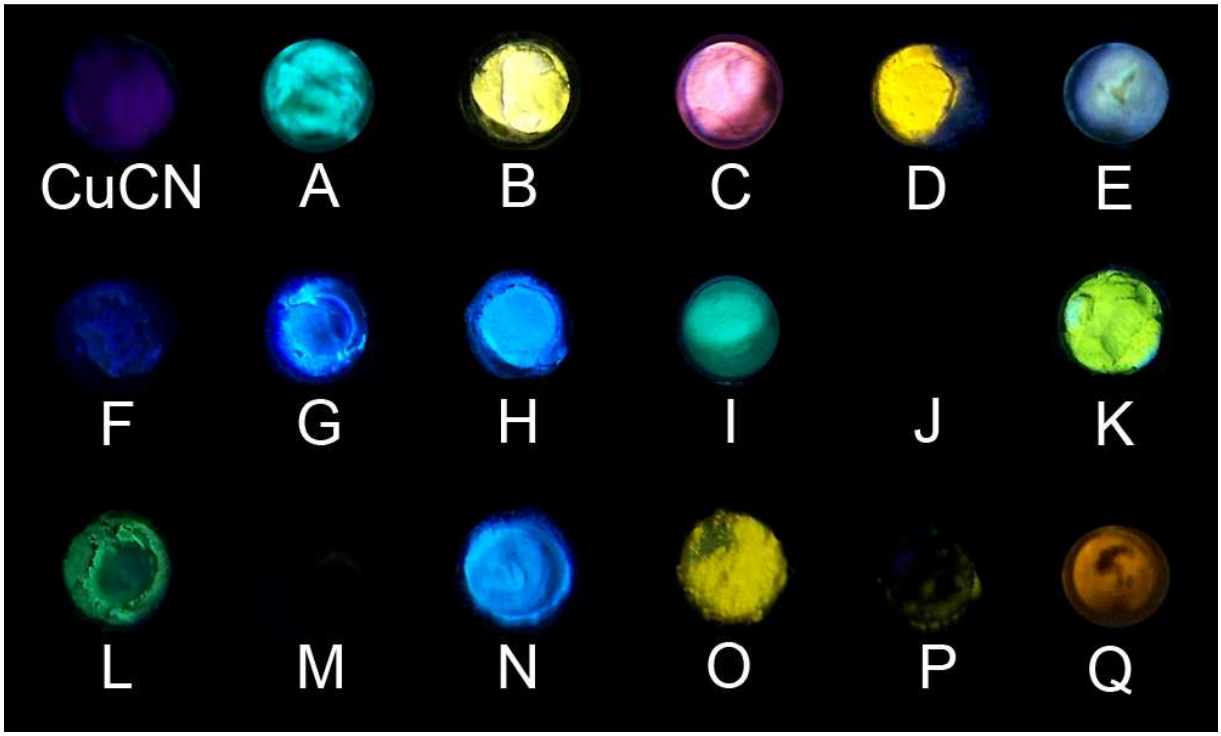

**Thermogravimetric Analysis**

Product stoichiometries were determined primarily through use of thermogravimetric analysis (TGA), which utilizes a microbalance to monitor sample mass in a furnace while the temperature is raised. By heating to 300 °C, the volatilization of bound amines was achieved without loss of CuCN, such that all the CuCN remained after all traces of amine had been vaporized. By comparing the final mass to the original sample mass, a percent weight of CuCN in the compound can be calculated, with the missing percentage attributed to the amine in the original product. A typical TGA trace is shown in Figure 13 below, which depicts the resulting graph after analysis of (CuCN)(3MePy).

Figure 13: Thermogravimetric Analysis Trace for (CuCN)(3MePy)

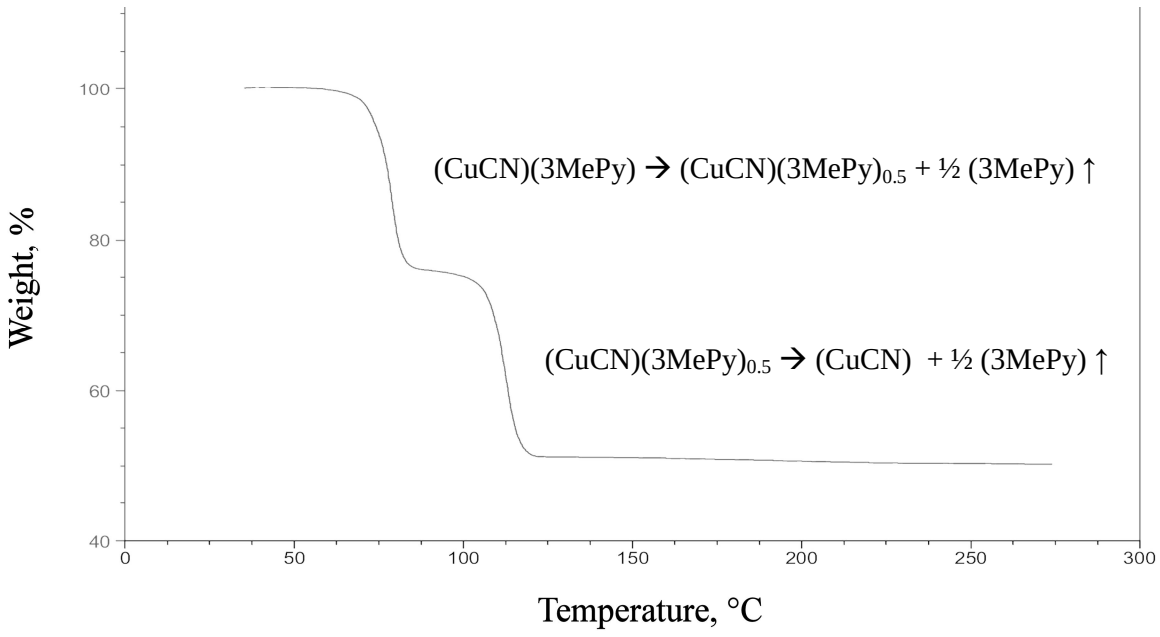

Table 1 shows a comprehensive list of the products that were isolated using the tube reaction method. In some cases, a unique stoichiometric compound was identified after allowing the initial product to remain on a vacuum line overnight. These 'vacuum products' are also identified in the table below and most often show a luminescence that differs from the initial product.

Table 1: Stoichiometries of Authentic CuCN-L Products from Tube Reactions.

| Ligand | Initial Product | Vacuum Product |
|---|---|---|
| Pyridine (Py) | **1a** (1:2) | **1b** (5:4) |
| 2-Methylpyridine (2MePy) | **2a** (2:3) | **2b** (1:1) |
| 2-Methylpyridine (3MePy) | **3a** (2:3) | **3b** (1:1) |
| 4-Methylpyridine (4MePy) | **4a** (2:3) | – |
| 2-Ethylpyridine (2EtPy) | **5** (1:1) | – |
| 3-Ethylpyridine (3EtPy) | **6a** (2:3) | **6b** (1:1) |
| 4-Ethylpyridine (4EtPy) | **7** (1:1) | – |
| 2-Chloropyridine (2ClPy) | **8a** (1:1) | – |
| 3-Chloropyridine (3ClPy) | **9a** (1:1) | – |
| 2-Bromopyridine (2BrPy) | **10a** (1:1) | – |
| 3-Bromopyridine (3BrPy) | **11** (1:1) | – |
| 4-tert-Butylpyridine (4$^{t}$BuPy) | **13a** (2:3) | – |
| 2,6-Lutidine (26Lut) | **14** (1:1) | – |
| 2,4,6-Collidene (246Coll) | **15** (1:1) | – |

| | | |
|---|---|---|
| Quinoline (Quin) | **16** (1:1) | – |
| Triethylamine ($NEt_3$) | **17a** (1:1) | – |
| Diethylamine ($NHEt_2$) | **18** (1:1) | – |
| Isopropylamine ($NH^iPr_2$) | **19** (2:1) | – |
| Piperidine (Pipd) | **20a** (3:4) | – |
| Methylpiperidine (MePipd) | **21a** (1:1) | – |
| Ethylpiperidine (EtPipd) | **22** (4:3) | – |
| Methylpyrollidene (MePyrrolid) | **23** (1:1) | – |
| Morpholine (Morph) | **24a** (2:3) | **24b** (1:1) |
| Methylmorpholine (MeMorph) | **25a** (1:1) | – |
| Dimethylcyclohexylamine ($NMe_2Cy$) | **26a** (1:1) | – |
| Dimethyl Sulfide ($Me_2S$) | **28** (3:1) | – |
| Tetrahydrothiophene (THT) | **29** (1:1) | – |

**Amine Exchange Reactions**

Some of the ligands from Table 1: 2,4,6-trimethylpyridine (246Coll) and quinoline (Quin) in particular, were found to undergo only partial reactions with CuCN by the tube method, failing to reach completion regardless of reaction time. To compensate, an exchange reaction method was developed in an effort to obtain authentic products for these ligands. It was thought that by initially reacting CuCN with excess pyridine, the spacing between neighboring CuCN chains could be increased by decorating the chains with pyridine ligands. It was hoped that teasing

apart the chains would ‘prime’ the CuCN network toward reaction with more sterically-hindered amines, such as Quin and 246Coll, that were blocked from interacting with the copper(I) centers prior to priming. Figure 14 illustrates the opening of the CuCN network by showing the structure before and after reaction with excess pyridine.

Figure 14: Spacing Effect of Pyridine on CuCN Networks. (A) Low Temperature Phase Copper(I) Cyanide Chain. Representations: Cu atoms, orange; disordered C/N atoms, gray.[13] (B) $(CuCN)_7(Py)_4$. Representations: Cu atoms, orange; C atoms, gray; N atoms, blue.[14]

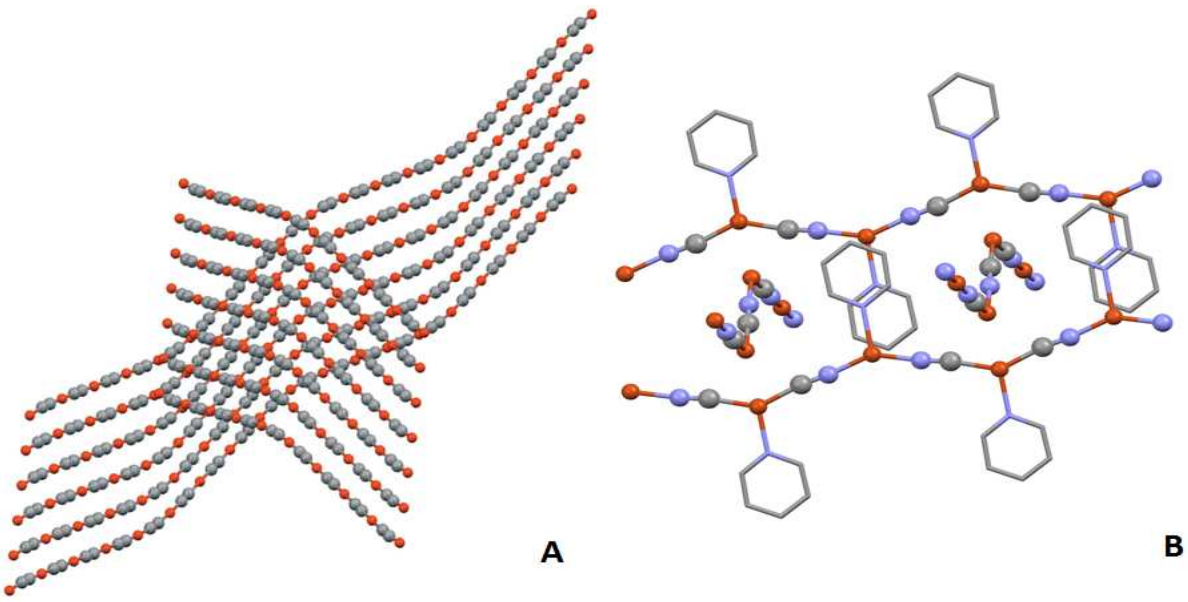


In the lab, the exchange reaction was performed by suspending CuCN in about 5 mL of neat liquid pyridine in a sealed pressure tube and reacting overnight under argon at 70 °C to create

$(CuCN)_5(Py)_4$ by the tube reaction method. Once this product was isolated, the exchange reaction was carried out using the same heated tube method. However, in this case $(CuCN)_5(Py)_4$ was used in place of the CuCN and was reacted with the neat liquid amine of interest. This sequence of the amine replacement reaction is presented in equations (1) and (2) below:

$$CuCN\ (s) + Py\ (l) \rightarrow (CuCN)_5(Py)_4\ (s) \quad (1)$$

$$(CuCN)_5(Py)_4 + L\ (l) \rightarrow (CuCN)_x(L)_y + Py \quad (2)$$

Using this method, TGA amine losses were found to be within acceptable ranges of the theoretical amine percent by weight, suggesting that complete reactions had been obtained. Exchange reaction results are summarized in Table 2 below:

Table 2: Comparison of Tube Reaction with Exchange Reaction Products.

| Product | Tube Reaction % CuCN | Exchange Reaction % CuCN | Theoretical % CuCN |
|---|---|---|---|
| (CuCN)(Quin) | 52.3% | 41.3% | 40.9% |
| (CuCN)(246Coll) | 65.8% | 42.4% | 42.5% |

**Powder X-Ray Diffraction**

To confirm that inclusion of amine into the CuCN network had indeed occurred, powder X-ray diffraction (PXRD) was used to obtain a characteristic diffraction pattern for the samples. PXRD was also used to determine whether powder products corresponded to those of solved single crystal structures. In order for X-ray diffraction to occur, the conditions of the Bragg equation (3) must be satisfied:

$$n\lambda = 2d \sin\theta \quad (3)$$

The n term is a harmonic value (typically 1) and $\lambda$ is the X-ray wavelength for a given source ($\lambda$ = 1.541 Å for the Cu radiation used for these determinations), both of which remain constant for a sample. Thus the determining factors are d, which is the spacing between atomic layers that cause diffraction, and $\theta$, the angle of both the incident and diffracted beam. In our instrument, a movable detector is used to capture the diffracted beams from the sample while the incident beam is kept stationary. Thus, the detector angle is the sum of both incident and diffraction angles $2\theta$. Equivalence of incident and diffraction angles is maintained by altering the sample stage angle. PXRD measures the diffraction angle, from which the d-spacing of a sample can be derived, with high angle peaks signifying a tightly packed network with small d-spacings, and low angle peaks indicative of larger d spacings.

A powder sample is different from a single crystal since it is composed of many crystallites randomly oriented in space. As a result of their orientation, only a handful of the crystals in a powder sample satisfy the Bragg equation and actually diffract the incoming X-rays at any given angle. To observe all possible diffraction directions of the crystal lattice, the sample is scanned through a range of detector angles ($2\theta$).

In our work, powder X-ray diffraction patterns were taken of the authentic products **(B)** and compared to several other variations, which included pure CuCN **(A)**; liquid-exposed samples **(C)** and vapor-diffused samples **(D)**. When these PXRD traces are overlaid, such as in Figure 15, the similarities in these products become much easier to compare.

The most noticeable difference is the appearance of low angle 2θ peaks in compounds that were exposed to amines, which is indicative of an increase in d-spacing via Bragg's Law. This observation is consistent with our model of amine inclusion into the powder structure, which would take up space between the planes in the atomic lattice and push them further apart, effectively increasing the d-spacing.

Furthermore, all amine products showed similar powder pattern characteristics with variations in peak intensity, most notably the leading lowest angle peak around 5° 2θ. This was present in authentic products, liquid-exposed samples, and vapor-diffused samples, suggesting that liquid-exposed and vapor-diffused products had interacted with the amines in the same manner as one would have observed in an authentic reaction to produce networks with similar d-spacings. An overlay of these PXRD traces for $(CuCN)_3(Pipd)_4$, is shown in Figure 15 below.

Figure 15: Powder X-Ray Diffraction Patterns for $(CuCN)_3(Pipd)_4$. (A) Pure CuCN = black, (B) authentic $(CuCN)_3(Pipd)_4$ = red, (C) Pipd liquid-exposed (CuCN)(Pipd) = blue, (D) Pipd vapor-diffused CuCN pellet = green.

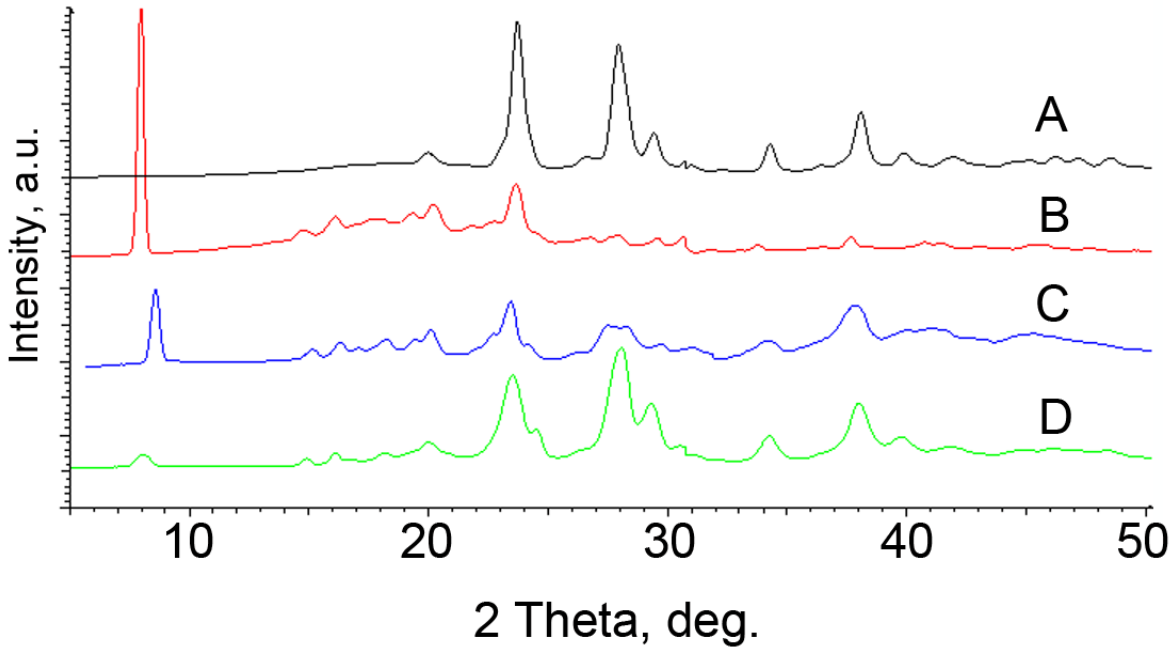

**Vial Reaction Products**

After reviewing the tube reaction products for some time, we decided to investigate the possibility of an alternative pathway to form similar products, but in a more consistent fashion. Referred to herein as vial reactions, these experiments were carried out by adding excess neat liquid amine to a two-dram vial containing CuCN powder under argon and allowing the suspension to stir for a period of three days at room temperature. The products collected were nearly identical to those from the tube reactions, with the exception of a lack of large crystal products. A summary of the vial products is given below, with comparisons made to the tube reactions. Product stoichiometries were mostly determined through use of TGA, however atomic absorption spectroscopy and elemental analysis were required to confirm some of the results that were not sufficiently clear.

Table 3: CuCN-L Product Stoichiometries by Comparison with Vial Reactions. See Experimental Section for interpretation of compound codes.

| Ligand | Tube Reaction | Vial Reaction |
|---|---|---|
| Py | $(CuCN)(Py)_2$ (**1a)** | $(CuCN)_2(Py)_3$ (**30**) |
| 2MePy | $(CuCN)_2(2MePy)_3$ (**2a**) | $(CuCN)_x(2MePy)_y$ **(31)** |
| 3MePy | $(CuCN)_2(3MePy)_3$ (**3a**) | $(CuCN)_3(3MePy)_2$ (**32**) |
| 4MePy | $(CuCN)_2(4MePy)_3$ (**4a**) | $(CuCN)_2(4MePy)_3$ (**33**) |
| 2EtPy | (CuCN)(2EtPy) (**5**) | (CuCN)(2EtPy) (**34**) |
| 3EtPy | $(CuCN)_2(3EtPy)_3$ (**6a**) | (CuCN)(3EtPy) (**35**) |

| | | |
|---|---|---|
| 2ClPy | (CuCN)(2ClPy) (**8a**) | $(CuCN)_3(2ClPy)_2$ (**36**) |
| 3ClPy | (CuCN)(3ClPy) (**9a**) | $(CuCN)_3(3ClPy)_4$ (**37**) |
| 2BrPy | (CuCN)(2BrPy) (**10a**) | (CuCN)(2BrPy) (**38**) |
| 3BrPy | (CuCN)(3BrPy) (**11**) | (CuCN)(3BrPy) (**39**) |
| 26Lut | (CuCN)(26Lut) (**14**) | (CuCN)(26Lut) (**40**) |
| 246Coll | (CuCN)(246Coll) (**15**) | (CuCN)(246Coll) (**41**) |
| Quin | (CuCN)(Quin) (**16**) | (CuCN)(Quin) (**42**) |
| $NEt_3$ | (CuCN)($NEt_3$) (**17a**) | $(CuCN)_3(NEt_3)$ (**43**) |
| $NHEt_2$ | (CuCN)($NHEt_2$) (**18**) | (CuCN)($NHEt_2$) (**44**) |
| Pipd | $(CuCN)_3(Pipd)_4$ (**20a**) | (CuCN)(Pipd) (**45**) |
| MePipd | (CuCN)(MePipd) (**21a**) | $(CuCN)_3(MePipd)_2$ (**46**) |
| EtPipd | $(CuCN)_4(EtPipd)_3$ (**22**) | $(CuCN)_4(EtPipd)_3$ (**47**) |
| MePyrrolid | (CuCN)(MePyrrolid) (**23**) | (CuCN)(MePyrrolid) (**48**) |
| Morph | $(CuCN)_2(Morph)_3$ (**24a**) | $(CuCN)_2(Morph)_3$ (**49**) |
| MeMorph | (CuCN)(MeMorph) (**25a**) | (CuCN)(MeMorph) (**50**) |
| $NMe_2Cy$ | (CuCN)($NMe_2Cy$) (**26a**) | $(CuCN)_3(NMe_2Cy)$ (**51**) |

Table 3 shows that many of the same compounds can be synthesized through this alternative room temperature vial reaction, but that in some cases different species are formed. Of particular interest is the product obtained when CuCN is reacted with 2MePy. When proceeding by the tube reaction method, the initial product is $(CuCN)_2(2MePy)_3$ which shows a vibrant yellow luminescence. During vacuum exposure, amine loss occurs, creating the reduced product of (CuCN)(2MePy), which shows a blue luminescence.

On the other hand, when following the vial reaction methodology, the final isolated compound shows a novel green luminescence that is clearly distinct from either of the two products formed through tube reactions. Curious as to the nature of this foreign compound, we launched several new studies, including PXRD to determine identity of this product, as well as more meticulous kinetic and thermodynamic studies of the reaction process for CuCN with 2MePy by vial reactions and vapor diffusion.

**Powder X-ray Diffraction**

Initial comparisons between PXRD patterns of the unknown sample and experimental patterns for the 1:1 and 2:3 products of (CuCN)(2MePy) supported the notion that the newly isolated compound displayed similar lattice spacing to those of the $(CuCN)_2(2MePy)_3$ compound. This is apparent in Figures 16 and 17 below.

Figure 16: Powder Pattern Overlay Comparison for $(CuCN)_x(2MePy)_y$ and (CuCN)(2MePy). Comparisons made between the unknown $(CuCN)_x(2MePy)_y$ compound (black) and the experimental pattern for (CuCN)(2MePy) (red).

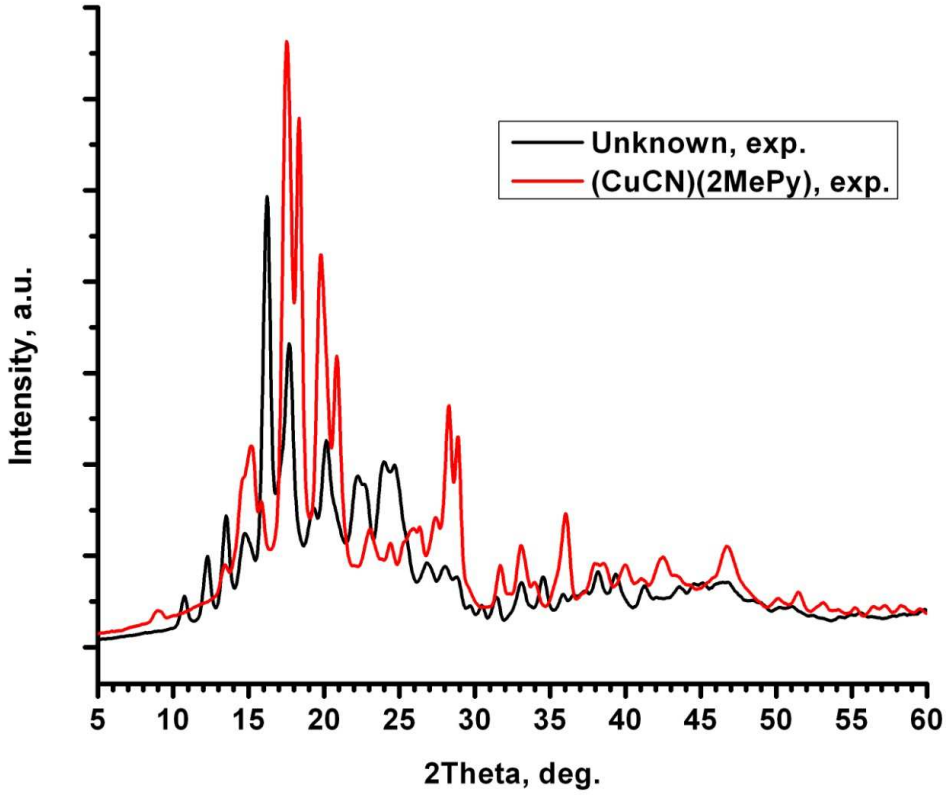

Figure 17: Powder Pattern Overlay Comparison for $(CuCN)_x(2MePy)_y$ and $(CuCN)_2(2MePy)_3$. Comparisons made between the unknown $(CuCN)_x(2MePy)_y$ compound (black) and the experimental pattern for $(CuCN)_2(2MePy)_3$ (red).

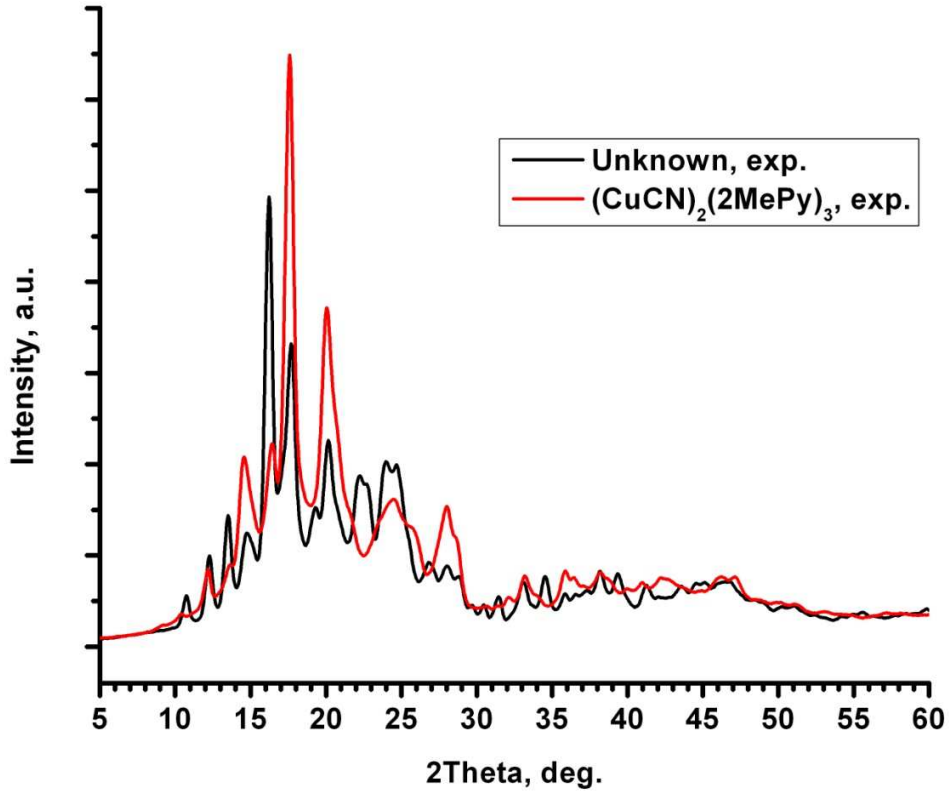


Fingerprint matches are analyzed based on 2θ similarities, as peak intensities for PXRD are not especially reliable since crystallographically preferred orientations can be present in powder samples. While the unknown fingerprint matches $(CuCN)_2(2MePy)_3$ very well, it is important to note that PXRD is a physical measure of d-spacing between lattice lines in a crystal and gives no chemical information. This can be extremely useful when using single crystal diffraction, which can be solved to give a detailed structural solution to the electron distribution corresponding to diffracted X-rays, but is more limited in the case of comparing PXRD fingerprints.

**Supplementary Characterization Techniques**

Not entirely convinced by the PXRD results, we wanted to support those findings using additional methods to confirm the identity of the unknown $(CuCN)_x(2MePy)_y$ product. Thermogravimetric analysis was the first test done and showed a plateau corresponding to 43.1% CuCN. When compared with (CuCN)(2MePy), which is theoretically composed of 49.0% CuCN, and $(CuCN)_2(2MePy)_3$, which has a theoretical composition of 39.0% CuCN, our numerical result was inconclusive. However, the TGA trace for $(CuCN)_2(2MePy)_3$ shows an additional loss at low temperatures that does not occur in (CuCN)(2MePy). Both of these TGA traces are shown in comparison to $(CuCN)_x(2MePy)_y$ in Figures 18 and 19 below.

Figure 18: TGA Overlay Comparison for $(CuCN)_x(2MePy)_y$ and (CuCN)(2MePy).
Overlay of (CuCN)(2MePy) TGA Trace (solid line) onto TGA Trace of $(CuCN)_x(2MePy)_y$ (dashed line)

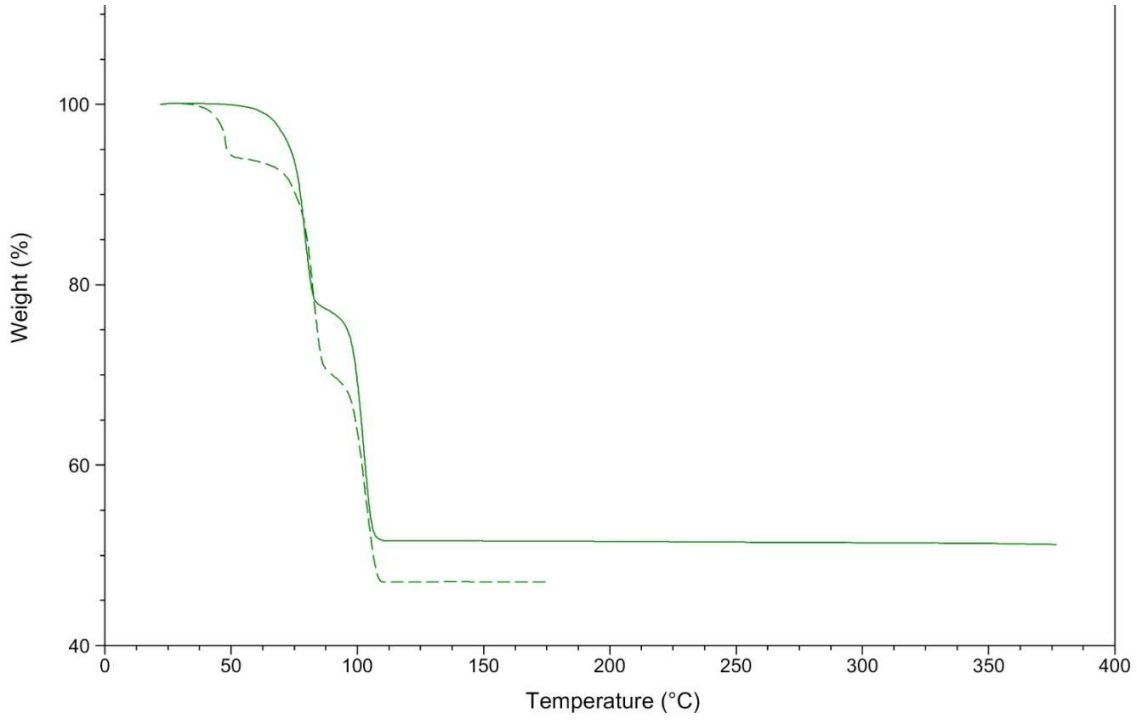

Figure 19: TGA Overlay Comparison for $(CuCN)_x(2MePy)_y$ and $(CuCN)_2(2MePy)_3$. Overlay of $(CuCN)_2(2MePy)_3$ TGA Trace (solid line) onto TGA Trace of $(CuCN)_x(2MePy)_y$ (dashed line)

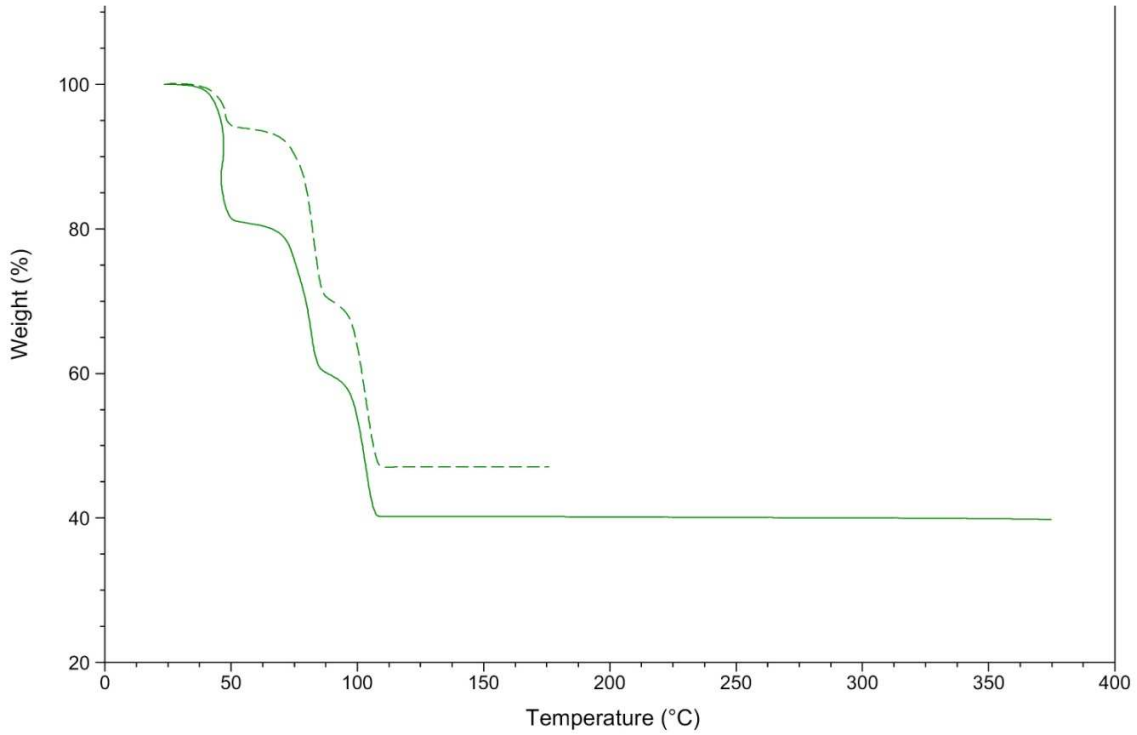


By comparison, a trace for the $(CuCN)_x(2MePy)_y$ compounds bears significant resemblance to $(CuCN)_2(2MePy)_3$ in terms of its number of decomposition steps during thermal volatilization of 2MePy. In fact, these traces are nearly identical, with only slight variations in the temperature range of amine vaporization and final mass percent of associated CuCN. Thus, these results also support the findings that $(CuCN)_x(2MePy)_y$ is similar in chemical constitution to $(CuCN)_2(2MePy)_3$ , but retains slight differences to create a unique luminescent product.

Finally, elemental analysis was run on the unknown compound in two forms to confirm composition of the sample: combustion analysis and atomic absorption spectroscopy. Combustion analysis uses a small sample (0.5–1.5 mg) that is burned in excess oxygen, with the resulting products collected by various traps. The masses of these products, which include carbon dioxide ($CO_2$), water ($H_2O$), and nitric oxide (NO), can then be used to calculate the percent composition of the unknown sample in terms of carbon, hydrogen, and nitrogen (this procedure is also commonly referred to as CHN analysis for this reason).

Atomic absorption measures the concentration of an analyte by relating measured absorbance in a sample to a set of standard solutions. To accomplish this, the sample is atomized in a high temperature air/acetylene flame and then subjected to optical radiation, which excites the released atoms. The absorption by these atoms decreases the amount of radiation reaching the detector, which can be translated into an interpretable signal. The change in signal can then be compared to a set of known standards to determine the percent of a particular element that may be present by using Beer's Law (4)

$$A = \varepsilon bc \tag{4}$$

Where A is the measured absorbance, ε is the molar absorptivity, an intrinsic property specific to a particular chemical species, b is the path length of the cell containing the sample, and c is the concentration of the sample. For our needs, a copper lamp was used as the radiation source so that we could determine the percent copper in our samples. The results for combustion analysis and atomic absorption spectroscopy of $(CuCN)_x(2MePy)_y$ are summarized in Table 4.

Table 4: Percent Composition for $(CuCN)_x(2MePy)_y$ by Element. The $(CuCN)_x(2MePy)_y$ sample shows experimental results, whereas the (CuCN)(2MePy) and $(CuCN)_2(2MePy)_3$ entries give theoretical values for elemental composition.

| **Compound** | **Carbon, %** | **Hydrogen, %** | **Nitrogen, %** | **Copper, %** |
|---|---|---|---|---|
| $(CuCN)_x(2MePy)_y$ | 44.42 | 4.01 | 15.68 | 32.2% |
| (CuCN)(2MePy) | 45.98 | 3.83 | 15.33 | 34.8% |
| $(CuCN)_2(2MePy)_3$ | 52.30 | 4.58 | 15.27 | 27.7% |

Based on comparisons of the data, namely percent of carbon, hydrogen, and copper in the compound, it is very clear that $(CuCN)_x(2MePy)_y$ resembles (CuCN)(2MePy), a finding contradictory to earlier observations. Since current attempts to isolate a single crystal of $(CuCN)_x(2MePy)_y$ for single crystal X-ray diffraction have been unsuccessful, we have been unable to conclude the true identity of the unknown compound based on our conflicting analytical results.

**Vapor Diffusion Studies**

Following the powder X-ray diffraction studies, we wished to distinguish between absorption and adsorption of the amines by the CuCN network when using the vapor diffusion mechanism. After exposure to gaseous amines, analysis of the powder samples were performed by TGA as described earlier to determine the extent of amine vapor uptake by CuCN powder. A TGA trace representative of these experiments is shown below in Figure 20, which shows results for an authentic sample of $(CuCN)_2(Morph)_3$ compared against a vapor diffusion sample of CuCN powder exposed to morpholine vapor.

Figure 20: TGA Traces for Authentic $(CuCN)_2(Morph)_3$ (A) and Vapor Diffusion of Morpholine onto CuCN Powder (B). Inset image shows a magnification of the temperature range from 37 ° C – 150 °C and the weight percent from 99.75% to 100.05% for the vapor diffusion sample only.

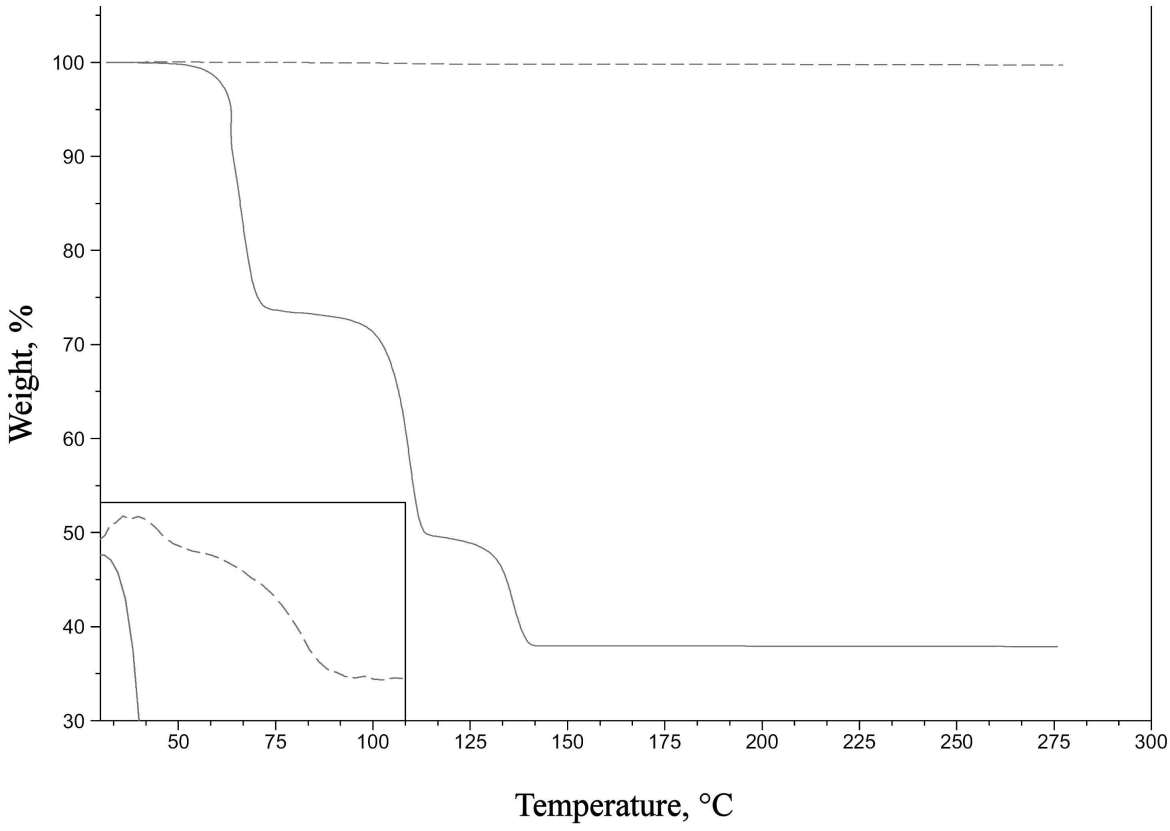

This study consistently showed that amine vapor mass uptake by CuCN was low, with amine percent by weight not exceeding 0.5% for an exposure time of twelve hours. Combined with the results from PXRD, which clearly showed the presence of amine in the isolated products, as well as general luminescent observations, a model for amine uptake by CuCN was constructed and is shown below in Scheme 1.

Scheme 1: Suggested Mechanism for the Uptake of Amines by Copper(I) Cyanide. The upper path shows the reaction parameters for an authentic tube reaction, the lower path for a vapor diffusion reaction.[5]

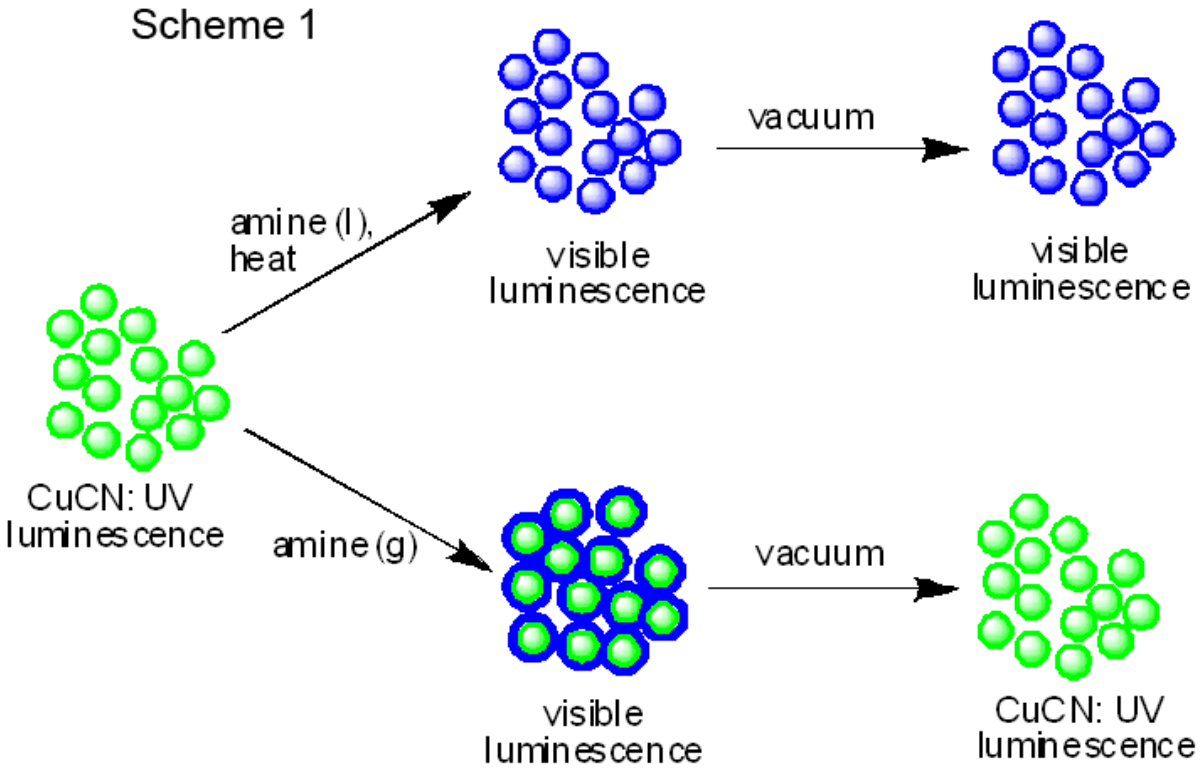

As outlined in Scheme 1, authentic tube reactions showed a change in visible luminescence that could not be entirely removed by vacuum and took up a significant weight percent of the total, which suggests absorption of the amine into the CuCN network. In contrast, vapor diffusion reactions produced a change in visible luminescence that was easily removed by vacuum and that took up an insignificant amount of weight percent of the total, which suggests an adsorption of amine onto the surface of CuCN.

**Kinetics**

Kinetic data were recorded for (CuCN)(2MePy) products over the course of nine days via the ambient temperature vial reaction process and for thirty-five days via vapor diffusion. The major products isolated during the vial reaction study are displayed below in Figure 21 and occur at twelve, twenty-four, and thirty-six hours. Data points were collected with TGA so that we could relate reaction time with the mole percent of amine taken up by CuCN. A plot of these kinetic data can be found in Figure 22.

Figure 21: Kinetic Study of CuCN–2MePy Products Isolated via Vial Reactions. A luminescence photograph of products isolated at varying time intervals during the kinetic study under 365 nm light: (A) (CuCN)(2MePy) collected at 12 hr, (B) $(CuCN)_2(MePy)_3$ collected at 24 hr, (C) Unknown $(CuCN)_x(2MePy)_y$ product collected at 36 hr.

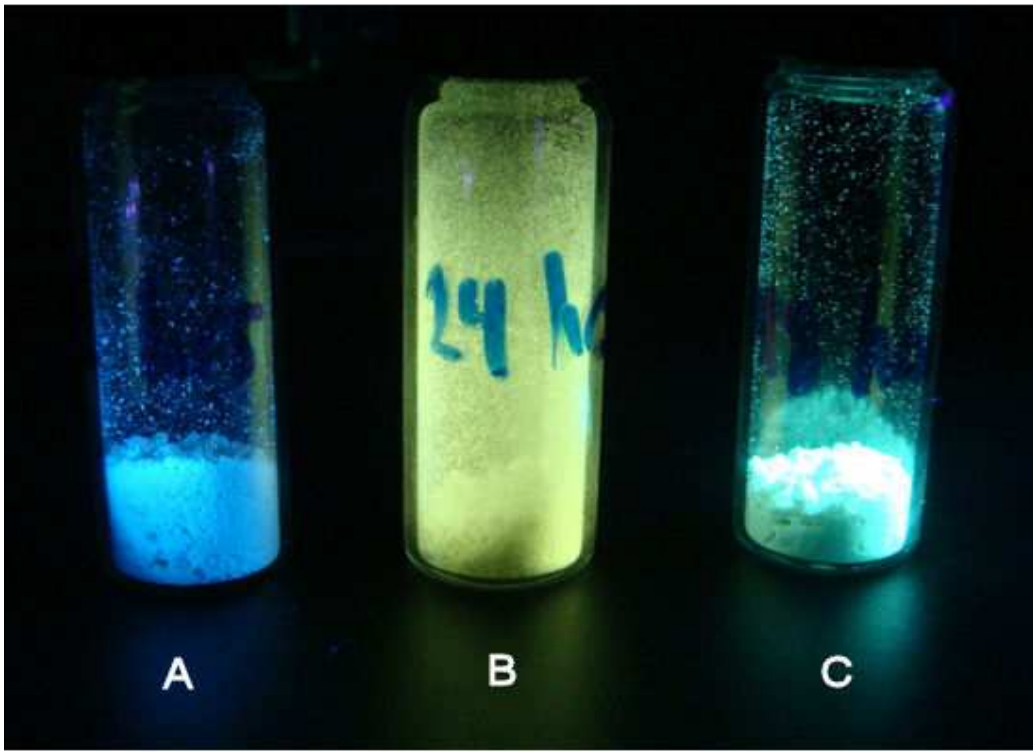

Figure 22: Vial Reaction Uptake of 2MePy by CuCN. This plot shows the take up of liquid 2MePy by CuCN following the vial reaction parameters, with asymptotic behavior around 0.60 mole fraction of 2MePy.

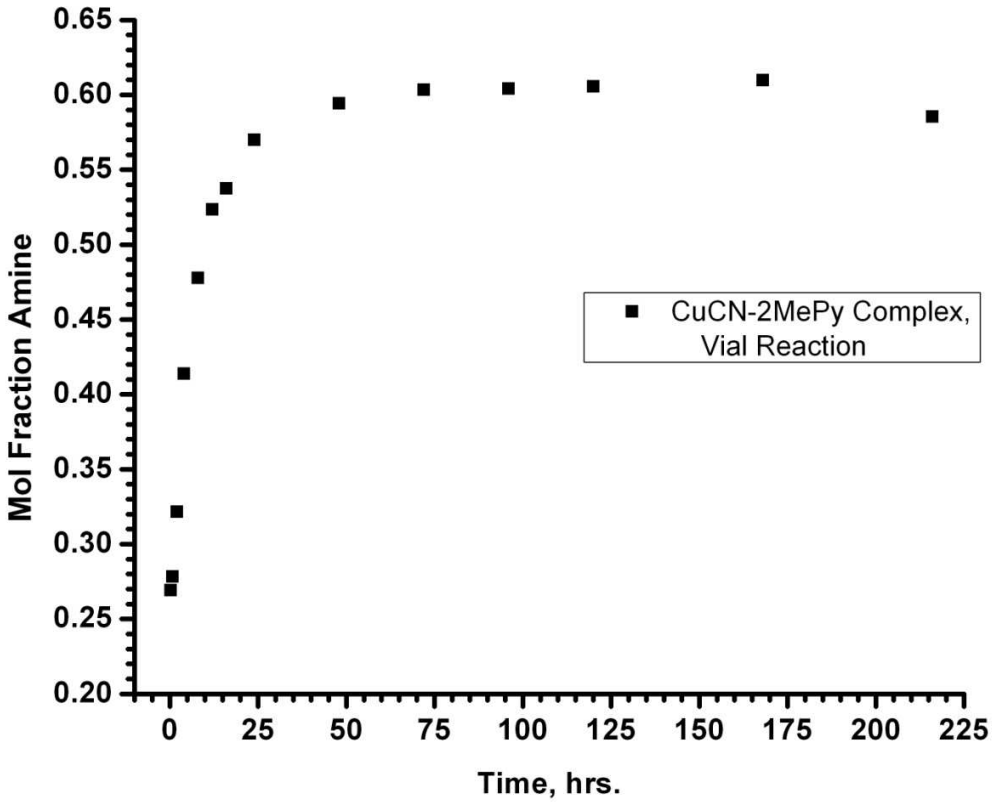


By comparison, only two unique products, (CuCN)(2MePy) and $(CuCN)_2(2MePy)_3$ were isolated by vapor diffusion, with plots for these data shown below in Figure 23.

Figure 23: Vapor Diffused Uptake of 2MePy by CuCN. This plot shows the take up of 2MePy vapors by CuCN following the vapor-diffused reaction parameters, with asymptotic behavior around 0.55 mole fraction of 2MePy.

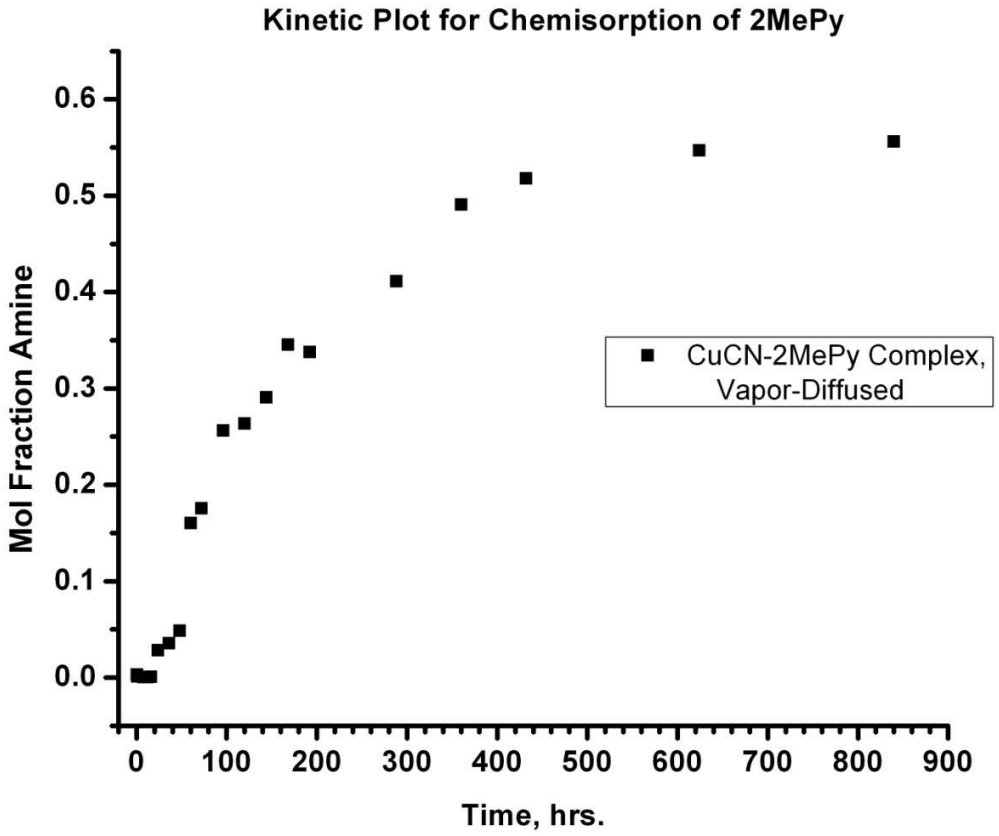


Comparing Figures 22 and 23 above, CuCN takes up 2MePy much more rapidly under liquid-exposed conditions rather than by vapor diffusion. Both processes also show asymptotes near the boundary for the formation of $(CuCN)_2(2MePy)_3$, which has a corresponding mole fraction of 0.61 for 2MePy.

**Thermodynamic Studies**

A thermodynamic product domain study was conducted using the heated tube reaction method, with twenty-four hours allotted to the establishment of reaction equilibrium. The results showed an interesting shift between the two known CuCN compounds of 2MePy. At lower temperatures, the major product was found to be $(CuCN)_2(2MePy)_3$, which shows a bright yellow luminescence, but at higher temperatures this shifted to (CuCN)(2MePy), which shows blue luminescence in response to UV excitation. The yellow 2:3 form appeared at temperatures less than or equal to 65.4 °C, whereas the blue 1:1 form was seen at temperatures greater than or equal to 65.7 °C. At the transitional temperatures between 65.4 °C and 65.7 °C, it appears that these two forms exist simultaneously, as indicated by a mixture of blue and yellow in the observed luminescence. These observations are summarized in Table 5 below, with Figure 24 displaying photographs of the different products within the determined boundaries.

Table 5: Thermodynamic Product Range for CuCN-2MePy Compounds.

| **Temperature Range** | **Observed Luminescence** | **Correlated Products** |
|---|---|---|
| 0 °C – 65.4 °C | Yellow | $(CuCN)_2(2MePy)_3$ |
| 65.5 °C – 65.6 °C | Yellow/Blue Mix | $(CuCN)_2(2MePy)_3$ and (CuCN)(2MePy) |
| 65.7 °C – 100 °C | Blue | (CuCN)(2MePy) |

Figure 24: Thermodynamic (CuCN)(2MePy) Products via Tube Reaction. (A) $(CuCN)_2(2MePy)_3$ observed from 0 °C to 65.4 °C, (B) a mixture of $(CuCN)_2(2MePy)_3$ and (CuCN)(2MePy) observed from 65.5 °C to 65.6 °C, (C) (CuCN)(2MePy) observed from 65.7 °C to 100 °C.

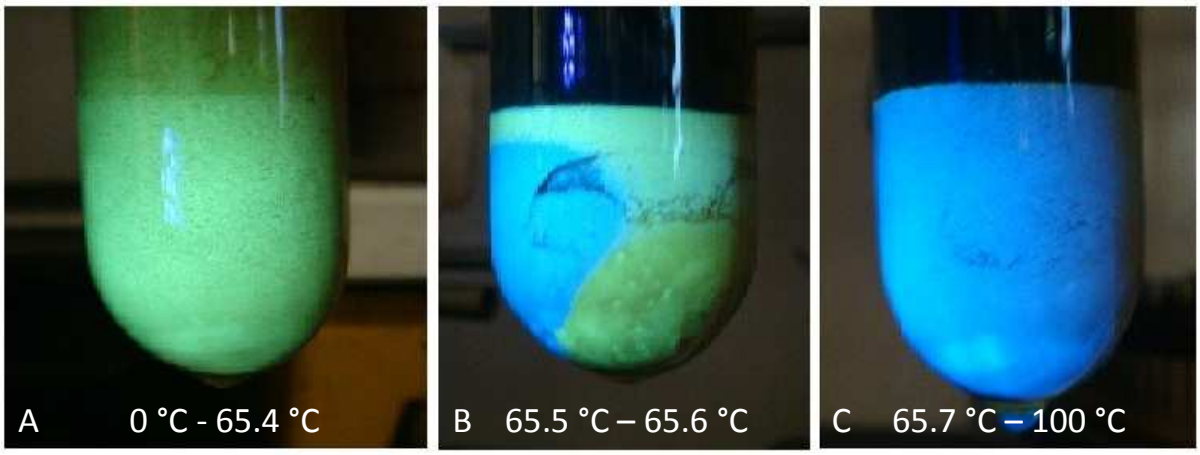


**Luminescent Spectra and Quantum Yields**

Noting that the synthesized CuCN-amine compounds were highly luminescent, we wished to quantify this phenomenon. This was accomplished using a spectrofluorimeter, which uses light to excite electrons in the sample molecule. The excited electrons then release the energy imparted to them by the source light in the form of photons as they eventually decay back down the ground state. During this relaxation process, the photonic emissions are observed using a detector, which is able to translate the photon flux into relative intensity. Both excitation and emission wavelengths can be independently varied. By scanning over a range of wavelengths (typically 250–450 nm for excitation and 400–800 nm for emission) a spectrum is compiled that relates the wavelength of light to the intensity of the detected emission. A sample spectrum is depicted in Figure 25.

Figure 25: Luminescent Spectrum for the (CuCN)(246Coll) Vial Product.

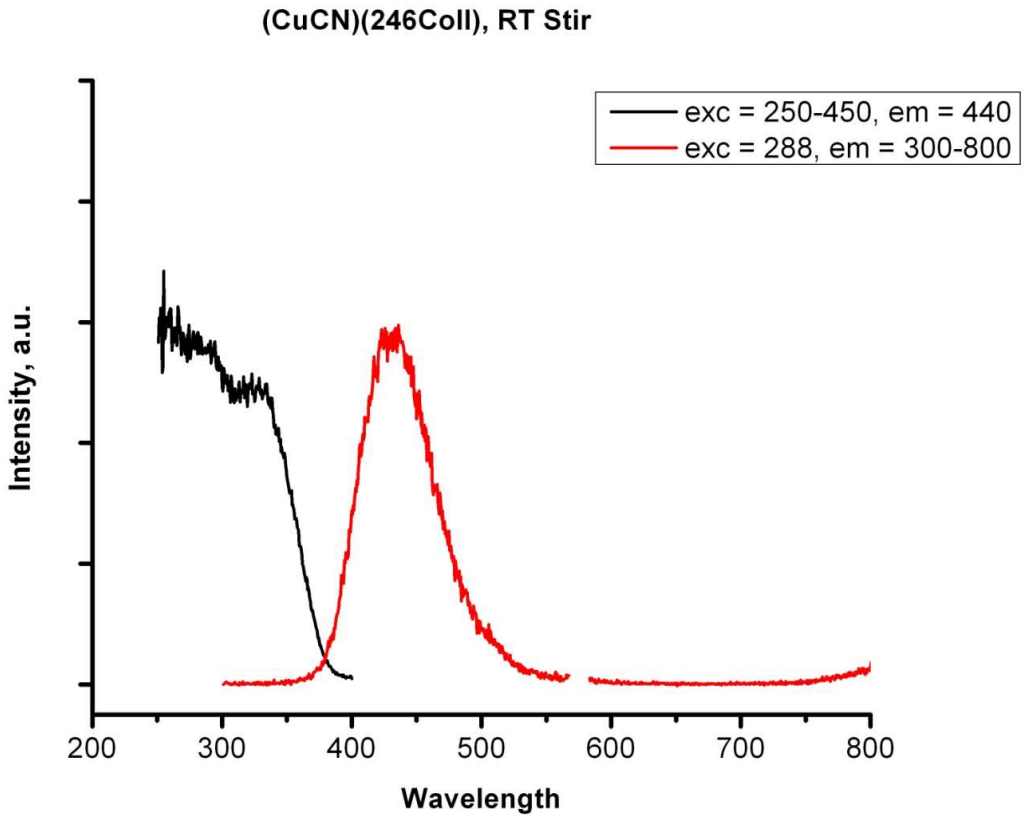


When operating the fluorimeter, one can determine the wavelength at which sample emission is the most intense by scanning emission at constant excitation wavelength. Next, the source excitation wavelength can be tweaked to give the highest emission possible by the sample: $\lambda_{max}$. Once the $\lambda_{max}$ is identified for both excitation and emission, quantum yield can be determined. Solid state quantum yield was determined using Mann's method.[10] Quantum yield is defined as the emission efficiency of the products, or more simply the number of photons emitted in comparison to the total number of photons absorbed by the sample, and is determined using Equation 5:

$$\varphi = \frac{I_{emit}}{I_0 - I} \tag{5}$$

Where φ is the calculated quantum yield, $I_{emit}$ is the intensity of the emission peak from the sample, $I_0$ is the intensity of the peak obtained from a perfect scatterer (Fluorilon was used for our calculations) and I is the intensity of the peak from a scan of a combination of the sample on top of the scatterer. A compilation of quantum yields for fluorescent products formed through the vial reaction method can be found in Table 6 below:

Table 6: Fluorescent Data for (CuCN)(L) Vial Reaction Products.

| Sample | $\lambda_{excitation}$, nm | $\lambda_{emission}$, nm | Quantum Yield, % |
|---|---|---|---|
| $(CuCN)(Py)_2$ | 254 | 507 | 10.1 |
| $(CuCN)_x(2MePy)_y$ | 288, 350 | 477 | 1.6 |
| (CuCN)(3MePy) | 289, 336 | 497 | 89.0 |
| (CuCN)(2EtPy) | 333 | 448 | <0.05 |
| (CuCN)(3BrPy) | 289, 330 | 518 | 0.4 |
| (CuCN)(26Lut) | 291, 329 | 438 | 17.7 |
| (CuCN)(246Coll) | 288, 333 | 440 | 18.1 |
| $(CuCN)(NEt_3)$ | 254, 303 | 440 | 4.5 |
| $(CuCN)(NHEt_2)$ | 263, 288 | 421 | <0.05 |
| $(CuCN)_3(Pipd)_4$ | 269, 319 | 482 | 14.6 |
| (CuCN)(MePipd) | 261, 297 | 445 | <0.05 |
| (CuCN)(MePyrrolid) | 281 | 539 | <0.05 |
| $(CuCN)_2(Morph)_3$ | 267 | 438 | 10.9 |
| (CuCN)(MeMorph) | 291, 359 | 394 | 3.1 |

Only samples that displayed homogenous luminescence could be analyzed for quantum yield; non-luminescent samples give no emission, and mixed luminescent samples show emission at more than one $\lambda_{max}$. The CuCN-amine quantum yields varied widely, with a typical sample showing about 15% emission efficiency. While a higher efficiency is more desirable, even the lower quantum yield products were highly visibly luminescent nonetheless and remain viable for use in a sensory system.

Quantum yield measures gave us another opportunity to compare the unknown $(CuCN)_x(2MePy)_y$ vial reaction product to the (CuCN)(2MePy) and $(CuCN)_2(2MePy)_3$ compounds from tube reactions. These data, show in Table 7, confirm that $(CuCN)_x(2MePy)_y$ displays a luminescence unique from the tube reaction CuCN-amine products, however all species are similar in their conversion of absorbed photonic energies.

Table 7: Luminescent Measures of CuCN-2MePy Compounds.

| **Compound** | **$\lambda_{excitation}$, nm** | **$\lambda_{emission}$, nm** | **Quantum Yield, %** |
|---|---|---|---|
| $(CuCN)_x(2MePy)_y$ | 364 | 490 | 1.64 |
| (CuCN)(2MePy) | 335 | 453 | 1.97 |
| $(CuCN)_2(2MePy)_3$ | 339 | 517 | 1.15 |

**Alternative Sensory Platforms:**

Having seen significant results from primary testing with powder reactants, the development of a viable sensory platform became our next goal. Since CuCN provided a luminescent, widely reactive sensory foundation, we wanted to develop a system that would be easy to produce, portable, and reusable. Ideally, we had hoped to find these characteristics in a solid state substrate, which led to investigations of CuCN pellets and CuCN impregnated polymer films as our primary candidates.

**CuCN Pellets**

Experiments were conducted on CuCN pellets with the hope that the pellets would maintain the same luminescent properties of CuCN powder while providing a solid, more uniform, compact surface to which adsorbents could adhere. Furthermore, by restricting interactions to the surface of CuCN, we hoped to make it easier to strip volatile ligands from the pellet by application of a vacuum, which would allow for an easy method of ligand removal and add a recyclable quality to the pellets. All pellets were created using an IR pellet press by following the procedure in the Experimental Section and were stored in a desiccator to prolong their lifetime. A typical observation is displayed below in Figure 26, which shows a CuCN pellet before and after exposure to amine vapors.

Figure 26: Amine Vapor Diffusion onto a CuCN Pellet. The following photographs display CuCN Pellets under 365 nm UV excitation: (A) CuCN pellet prior to exposure. (B) CuCN pellet after six hours in a 2MePy saturated atmosphere. (C) CuCN pellet from (B) after 24 hours under vacuum. (D) CuCN pellet from (B) after six days under vacuum.

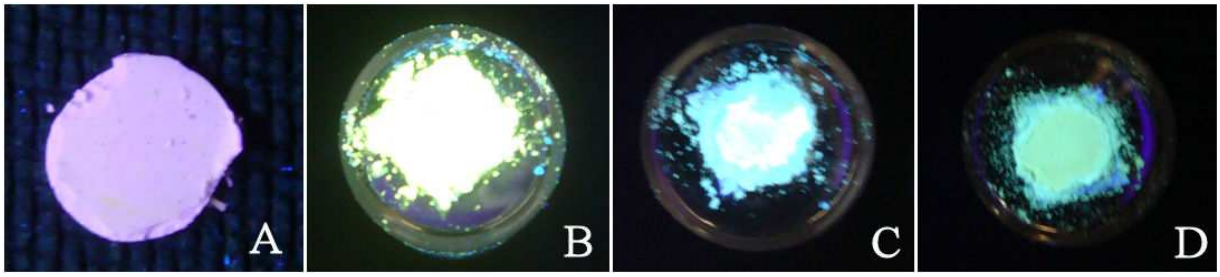


As shown above, vapor diffusion onto the pellet platform met with limited success. While luminescent changes were readily apparent with exposure to gaseous amine, removal of the amines under vacuum proved to be quite difficult. Diffusion proceeded directly to a yellow luminescence product, which is typically representative of $(CuCN)_2(2MePy)_3$, as shown in Photo (B). Photo (C) denotes a reduction to (CuCN)(2MePy) after 24 hours under vacuum with corresponding reduction in luminescent intensity (D). Nevertheless, the original state in (A) was not reached under vacuum.

Given these observations, it seems that pellets may not be reusable; however that does not eliminate them as a viable sensory platform. They are very quickly produced (< 2 minutes) and use no chemical materials aside from CuCN powder, and so may still be useful as a disposable means of vapor detection.

**CuCN Impregnated Polymer Films**

Also of interest for sensory applications was the development of a polymer film that could serve to carry CuCN. This was successfully accomplished by suspending CuCN in a solution of PVC before casting the film, as described Experimental Section. Microscopy pictures of the films in Figure 27 show that CuCN was indeed embedded in the cured polymer films, using between 0.25:1 and 1:1 CuCN to PVC ratio by weight.

Figure 27: Microscopic Images of CuCN-impregnated PVC Films. (A) 0.25:1 (CuCN:PVC by weight) film, (B) 0.5:1 film, (C) 0.75:1 film, (D), 1:1 film.

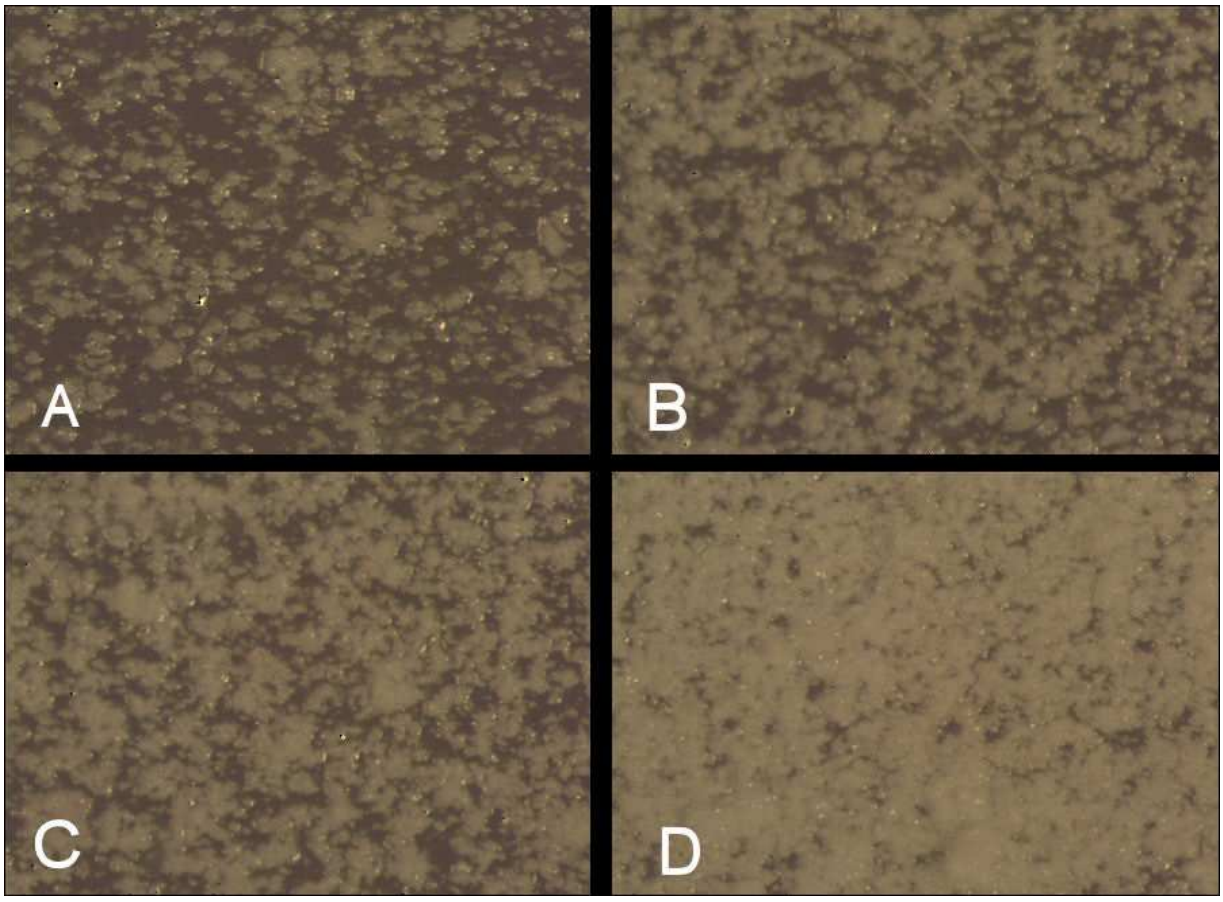

Initial testing methods involved drop tests with various liquid amines, however this proved degradative to the films, which appeared to be somewhat soluble in the liquid amines, and few results were produced. Vapor diffusion was attempted next and showed results typical of an authentic reaction while leaving the films essentially intact, physically. This is exemplified in Figure 28, which shows luminescence testing results for 2-methylpyridine diffusion onto a 1:1 CuCN-PVC film.

Figure 28: CuCN-impregnated PVC Films under 365 nm UV Light. (A) 1:1 (CuCN:PVC) polymer film. (B) 1:1 polymer film after six hours exposure to 2MePy vapors (C) 1:1 film from (B) after vacuum drying.

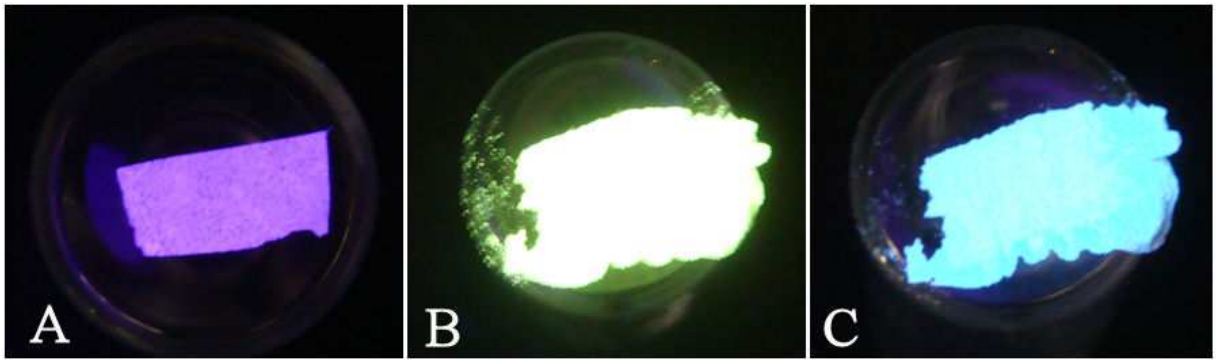


As was noted with pellets, it seems that CuCN films also retain amines very well. The films first sign of amine adsorption occurred after four hours, showing a mix of blue and yellow luminescence. Within six hours of exposure time, the film had become fully saturated and converted to an entirely yellow luminescence (B). While placing the sample under vacuum did

remove some amine from the film, it was unable to return the film to its original, pre-diffusion state (C).

These results would limit a CuCN film platform to use as a disposable detector. However the creation of these films is a lengthy process and requires multiple starting materials, making it less attractive than the pellet system. On the other hand, polymer films are more easily handled and presumably less toxic than crystalline CuCN, hence they might still be valuable given the right application.

# CONCLUSION

We have explored the formation of CuCN metal-organic networks containing amine and imine ligands by the vial reaction method. Comparisons with the previously-studied tube reaction method show that products from the two processes are often, but not always, identical. Most importantly, vial reaction products retain the remarkable luminescence behavior observed in tube reactions while at the same time showing a more consistent product formation.

The ligand-induced CuCN emission shift from the UV-visible border into the visible region offers wonderful potential for CuCN to serve as the foundation for a luminescent sensor system to detect amines or other nucleophilic VOCs. This observation held true for both liquid-exposed and vapor-diffused products, offering possibility for detection of VOCs in multiple phases. Additionally, the chemisorption of amines was found to be reversible with exposure to vacuum, a characteristic that would greatly extend the use of CuCN as a luminescent sensor.

Investigations of alternative sensory platforms for CuCN showed a loss of some of the more desirable characteristics of a sensor present in CuCN, but remain valuable nonetheless. CuCN pellets are quick to produce and provide a compact, portable system that was reactive to both liquid and gaseous amines. Observed luminescence was comparable to that seen in the synthesis of CuCN-amine networks, however we were unable to remove the associated amine with vacuum exposure.

In contrast, CuCN impregnated polymer films take much longer to produce than CuCN pellets, however are also presumably less toxic to handle. This system also showed uptake of gaseous amines, however exposure to liquid amines was degradative to the films. Chemisorption onto

films was also found to be irreversible with exposure to vacuum and would limit films to use as a disposable detector system.

**REFERENCES**


1) Araki, H.; Tsuge, K.; Sasaki, Y.; Ishizaka, S.; Kitamura, N. *Inorganic Chemistry* **2005**, *44*, 9967.
2) Armaroli, N.; Accorsi, G.; Cardinali, F.; Listorti, A. *Topics in Current Chemistry* **2007**, *280*, 69.
3) Schatz, M.; Becker, M.; Thaler, F.; Hampel, F.; Schindler, S.; Jacobson, R.; Tyeklar, Z.; Murthy, N.; Ghosh, P.; Chen, Q.; Zubieta, J.; Karlin, K. *Inorganic Chemistry* **2001**, *40*, 2312.
4) Hibble, S. J.; Eversfield, S. G.; Cowley, A. R.; Chippindale, A. M. *Angewandte Chemie International Edition* **2004**, *43*, 628.
5) Ley, A. N.; Dunaway, L. E.; Brewster, T. P.; Dembo, M. D.; Harris, T. D.; Baril-Robert, F.; Li, X.; Patterson, H. H.; Pike, R. D. *Chemical Communications* **2010**, *46*, 4565.
6) Horvath, A.; Stevenson, K. L. *Inorganic Chemistry* **1994**, *33*, 5351.
7) Ford, P. C.; Cariati, E.; Bourassa, J. *Chemical Reviews* **1999**, *99*, 3625.
8) Bayse, C. A.; Brewster, T. P.; Pike, R. D. *Inorganic Chemistry* **2009**, *48*, 174.
9) Wang, J.; Liu, H.; Ha, C. *Tetrahedron* **2009**, *65*, 9686.
10) McGee, K. A.; Veltkamp, D. J.; Marquardt, B. J.; Mann, K. R. *Journal of the American Chemical Society* **2007**, *129*, 15092.
11) Drew, S.; Smith, L.; McGee, K.; Mann, K. *Chemistry of Materials* **2009**, *21*, 3117.
12) Dembo, M. D.; Dunaway, L. E.; Jones, J. S.; Lepekhina, E. A.; McCullough, S. M.; Ming, J. L.; Li, X.; Baril-Robert, F.; Patterson, H. H.; Bayse, C. A.; Pike, R. D. *Inorganica Chimica Acta* **2010**, *364*, 102.

13) Hibble, S. J.; Cheyne, S. M.; Hannon, A. C.; Eversfield, S. G. *Inorganic Chemistry* **2002**, *41*, 4990.

14) (a) Pyykkö, P. *Chemical Reviews* **1997**, *97*, 597. (b) Hermann, H. L.; Bosch, G.; Schwerdtfeger, P. *Chemistry – A European Journal* **2001**, *7*, 5334.